



# AKAP18 $\delta$ Anchors and Regulates CaMKII Activity at Phospholamban-SERCA2 and RYR

Cathrine R. Carlson<sup>1</sup>, Jan Magnus Aronsen, Anna Bergan-Dahl<sup>1</sup>, Marie Christine Moutty, Marianne Lunde, Per Kristian Lunde, Hilde Jarstadmarken, Pimthanya Wanichawan, Laetitia Pereira, Terje R.S. Kolstad<sup>1</sup>, Bjørn Dalhus<sup>1</sup>, Hariharan Subramanian, Susanne Hille, Geir Christensen, Oliver J. Müller<sup>1</sup>, Viacheslav Nikolaev<sup>1</sup>, Donald M. Bers<sup>1</sup>, Ivar Sjaastad, Xin Shen, William E. Louch<sup>1</sup>, Enno Klussmann<sup>1</sup>, Ole M. Sejersted<sup>1</sup>

**BACKGROUND:** The sarcoplasmic reticulum (SR) Ca<sup>2+</sup>-ATPase 2 (SERCA2) mediates Ca<sup>2+</sup> reuptake into SR and thereby promotes cardiomyocyte relaxation, whereas the ryanodine receptor (RYR) mediates Ca<sup>2+</sup> release from SR and triggers contraction. Ca<sup>2+</sup>/CaMKII (CaM [calmodulin]-dependent protein kinase II) regulates activities of SERCA2 through phosphorylation of PLN (phospholamban) and RYR through direct phosphorylation. However, the mechanisms for CaMKII $\delta$  anchoring to SERCA2-PLN and RYR and its regulation by local Ca<sup>2+</sup> signals remain elusive. The objective of this study was to investigate CaMKII $\delta$  anchoring and regulation at SERCA2-PLN and RYR.

**METHODS:** A role for AKAP18 $\delta$  (A-kinase anchoring protein 18 $\delta$ ) in CaMKII $\delta$  anchoring and regulation was analyzed by bioinformatics, peptide arrays, cell-permeant peptide technology, immunoprecipitations, pull downs, transfections, immunoblotting, proximity ligation, FRET-based CaMKII activity and ELISA-based assays, whole cell and SR vesicle fluorescence imaging, high-resolution microscopy, adenovirus transduction, adenoassociated virus injection, structural modeling, surface plasmon resonance, and alpha screen technology.

**RESULTS:** Our results show that AKAP18 $\delta$  anchors and directly regulates CaMKII $\delta$  activity at SERCA2-PLN and RYR, via 2 distinct AKAP18 $\delta$  regions. An N-terminal region (AKAP18 $\delta$ -N) inhibited CaMKII $\delta$  through binding of a region homologous to the natural CaMKII inhibitor peptide and the Thr17-PLN region. AKAP18 $\delta$ -N also bound CaM, introducing a second level of control. Conversely, AKAP18 $\delta$ -C, which shares homology to neuronal CaMKII $\alpha$  activator peptide (N2B-s), activated CaMKII $\delta$  by lowering the apparent Ca<sup>2+</sup> threshold for kinase activation and inducing CaM trapping. While AKAP18 $\delta$ -C facilitated faster Ca<sup>2+</sup> reuptake by SERCA2 and Ca<sup>2+</sup> release through RYR, AKAP18 $\delta$ -N had opposite effects. We propose a model where the 2 unique AKAP18 $\delta$  regions fine-tune Ca<sup>2+</sup>-frequency-dependent activation of CaMKII $\delta$  at SERCA2-PLN and RYR.

**CONCLUSIONS:** AKAP18 $\delta$  anchors and functionally regulates CaMKII activity at PLN-SERCA2 and RYR, indicating a crucial role of AKAP18 $\delta$  in regulation of the heartbeat. To our knowledge, this is the first protein shown to enhance CaMKII activity in heart and also the first AKAP (A-kinase anchoring protein) reported to anchor a CaMKII isoform, defining AKAP18 $\delta$  also as a CaM-KAP.

**GRAPHIC ABSTRACT:** A graphic abstract is available for this article.

**Key Words:** calmodulin ■ calcium-calmodulin-dependent protein kinase type 2 ■ myocytes, cardiac ■ phospholamban ■ ryanodine receptor ■ sarcoplasmic reticulum calcium-transporting ATPases

In This Issue, see p 2 | Meet the First Author, see p 3 | Editorial, see p 45

In cardiac myocytes, Ca<sup>2+</sup> cycling is centrally involved in excitation-contraction coupling (ECC).<sup>1</sup> In this process, Ca<sup>2+</sup> enters the cell through L-type Ca<sup>2+</sup>

channels leading to the opening of ryanodine receptors (RYRs) in the sarcoplasmic reticulum (SR), and release of Ca<sup>2+</sup> (Ca<sup>2+</sup>-induced Ca<sup>2+</sup> release). The resulting

Correspondence to: Cathrine R. Carlson, Institute for Experimental Medical Research, Oslo University Hospital, Kirkeveien 166, N-0407 Oslo, Norway. Email cathrine.carlson@medisin.uio.no

Supplemental Material is available at <https://www.ahajournals.org/doi/suppl/10.1161/CIRCRESAHA.120.317976>

For Sources of Funding and Disclosures, see page 42.

© 2021 The Authors. *Circulation Research* is published on behalf of the American Heart Association, Inc., by Wolters Kluwer Health, Inc. This is an open access article under the terms of the [Creative Commons Attribution Non-Commercial-NoDerivs](https://creativecommons.org/licenses/by-nc-nd/4.0/) License, which permits use, distribution, and reproduction in any medium, provided that the original work is properly cited, the use is noncommercial, and no modifications or adaptations are made.

*Circulation Research* is available at [www.ahajournals.org/journal/res](http://www.ahajournals.org/journal/res)

## Novelty and Significance

### What Is Known?

- Sarcoplasmic/endoplasmic reticulum Ca<sup>2+</sup>-ATPase 2 (SERCA2) and ryanodine receptor (RZR) are essential for cardiac excitation-contraction coupling.
- Ca<sup>2+</sup>/CaMKII (CaM [calmodulin]-dependent protein kinase II) modulates SERCA2 and RZR activities through indirect and direct phosphorylation events, respectively, but CaMKII anchoring and local regulation mechanisms remain elusive.
- AKAP18 $\delta$  (A-kinase anchoring protein 18 delta) anchors protein kinase A to SERCA2-PLN (phospholamban).

### What New Information Does This Article Contribute?

- AKAP18 $\delta$  anchors and functionally regulates CaMKII activity at SERCA2-PLN and RZR, indicating a crucial role of AKAP18 $\delta$  in heartbeat regulation.
- AKAP18 $\delta$  also anchors CaM, inducing a second level of control.
- AKAP18 $\delta$  is the first AKAP reported to anchor a CaMKII isoform, defining AKAP18 $\delta$  as a CaM-Kinase Anchoring Proteins (CaM-KAP).

SERCA2 mediates Ca<sup>2+</sup> reuptake into SR and thereby promotes cardiomyocyte relaxation, whereas RZR mediates Ca<sup>2+</sup> release from SR and triggers contraction. CaMKII $\delta$  regulates activities of SERCA2, through phosphorylation of PLN, and RZR by direct phosphorylation. However, the mechanisms for CaMKII $\delta$  anchoring to SERCA2-PLN and RZR and its regulation by local Ca<sup>2+</sup> signals remain unclear. Here, we provide mechanistic insight into the anchoring and regulation of CaMKII $\delta$  activity by AKAP18 $\delta$  at SERCA2-PLN and RZR. We identified 2 unique regions in AKAP18 $\delta$  that inversely regulate CaMKII $\delta$  activity (CaMKII $\delta$ -catalyzed phosphorylation of Thr17-PLN and Ser2814-RZR) and SERCA2 and RZR function. We specifically showed that an inhibitory domain (AKAP18 $\delta$ -N) also binds calcified CaM, while an activating domain (AKAP18 $\delta$ -C) wedges CaMKII $\delta$  open, trapping CaM within the kinase, and lowering the Ca<sup>2+</sup> threshold for its activation. Based on our data, we propose a working model where the 2 unique AKAP18 $\delta$  regions fine-tune Ca<sup>2+</sup>-frequency-dependent activation of CaMKII $\delta$  at SERCA2-PLN and RZR. The peptide sequences derived from the 2 AKAP18 $\delta$  regions should be viewed as novel reagents that may help identify new CaMKII targets and approaches to therapeutically modify CaMKII activity and cardiomyocyte Ca<sup>2+</sup> cycling.

## Nonstandard Abbreviations and Acronyms

<b>AKAP</b>	A-kinase anchoring protein
<b>AKAP18<math>\delta</math></b>	A-kinase anchoring protein 18 $\delta$
<b>CaM</b>	calmodulin
<b>CaM-KAP</b>	CaM-kinase anchoring protein
<b>CaMKII</b>	Ca <sup>2+</sup> /calmodulin-dependent protein kinase II
<b>ECC</b>	excitation-contraction coupling
<b>GST</b>	glutathione S-transferase
<b>PDE3A1</b>	phosphodiesterase 3A1
<b>PKA</b>	protein kinase A
<b>PLN</b>	phospholamban
<b>RZR</b>	ryanodine receptor
<b>SERCA2</b>	sarco/endoplasmic reticulum Ca <sup>2+</sup> -ATPase 2
<b>SPR</b>	surface plasmon resonance
<b>SR</b>	sarcoplasmic reticulum

increase in intracellular Ca<sup>2+</sup> concentration ([Ca<sup>2+</sup>]) causes Ca<sup>2+</sup> binding to troponin C and activation of the myofilaments leading to contraction. For diastolic relaxation to occur, Ca<sup>2+</sup> is removed from cytoplasm by the

SR Ca<sup>2+</sup>-ATPase 2 (SERCA2), and to a lesser extent by the Na<sup>+</sup>/Ca<sup>2+</sup> exchanger. Alterations in this Ca<sup>2+</sup> cycling are associated with decreased contractility and arrhythmia during heart failure.<sup>2</sup>

Ca<sup>2+</sup>/CaMKII $\delta$  (CaM [calmodulin]-dependent protein kinase  $\delta$ ), which is the predominant CaMKII isoform expressed in heart, regulates ECC by phosphorylating several Ca<sup>2+</sup> handling proteins, including RZR and PLN (phospholamban).<sup>3</sup> PLN is a key modulator of SERCA2, and thus SR Ca<sup>2+</sup> reuptake, SR Ca<sup>2+</sup> load, and cardiomyocyte relaxation. Dephosphorylated PLN inhibits SERCA2 activity, whereas PLN phosphorylation at Thr17 by CaMKII $\delta$  (or Ser16 by PKA [protein kinase A]) reduces PLN interaction with SERCA2 and relieves this inhibition.<sup>4</sup> Likewise, phosphorylation at Ser2814-RZR by CaMKII $\delta$  increases RZR Ca<sup>2+</sup> sensitivity, leading to augmented SR Ca<sup>2+</sup> release and cardiomyocyte contraction. Inhibition of SR CaMKII $\delta$  activity results in decreased phosphorylation of RZR and PLN, and associated changes in Ca<sup>2+</sup> homeostasis and cardiac contractility.<sup>5</sup> These data support a pivotal role of CaMKII $\delta$  in fine-tuning ECC.

CaMKII forms a dodecamer that comprises 2 stacked 6-fold symmetrical rings.<sup>6</sup> The CaMKII monomer contains an N-terminal ATP-binding pocket, catalytic and autoregulatory domains, and a C-terminal association

domain mediating its oligomerization.<sup>7</sup> When CaMKII $\delta$  is in its inactive state, the Thr287 segment (Thr286 in CaMKII $\alpha$ ) in the autoregulatory domain binds to the so-called T-site in catalytic domain. This positions the adjacent sequence (pseudosubstrate) in the substrate-binding site (S-site) and ATP-binding pocket<sup>7</sup> (Figure S1A). Upon activation, Ca<sup>2+</sup>/CaM binds to the CaM-binding site in the autoregulatory domain, displacing the Thr287 segment from the T-site (Figure S1B) and enabling the kinase to be phosphorylated by a neighboring active (open) CaMKII $\delta$  molecule. Thus, binding of at least 2 CaM molecules is required for CaMKII autophosphorylation. Autophosphorylation of Thr287 increases CaMKII affinity for CaM,<sup>8</sup> maintains the kinase in an autonomously active state<sup>9</sup> (Figure S1C), and permits the kinase to translate the frequency of Ca<sup>2+</sup> spikes into kinase activity *in vitro*,<sup>10</sup> a form of molecular memory or integration.

Although CaMKII $\delta$  regulates several aspects of ECC, it remains unclear how the kinase is functionally regulated within the distinct nanodomains where these Ca<sup>2+</sup> handling proteins are localized. For example, local [Ca<sup>2+</sup>] near the PLN-SERCA2 complex is expected to be too low to appreciably activate CaMKII, while CaMKII near RYRs in the dyadic cleft should be activated by the much higher local [Ca<sup>2+</sup>] levels.<sup>11</sup> Although activated CaMKII $\delta$  in myocytes is more mobile than traditionally thought,<sup>12</sup> another potential explanation for PLN phosphorylation by CaMKII $\delta$  is that as yet unidentified CaMKAPs (CaM-kinase anchoring proteins) could enable locally higher Ca<sup>2+</sup> sensitivity of the kinase.

We postulated that the A-kinase anchoring protein, AKAP18 $\delta$  (also known as AKAP7 $\delta$ ), could perform such a CaMKII $\delta$  anchoring and regulatory role at PLN-SERCA2 and RYR. Originally identified in rat kidney,<sup>13</sup> AKAP18 $\delta$  has been shown to interact directly with PKA and PLN, thereby enabling PKA-dependent phosphorylation at Ser16-PLN and augmentation of SERCA2 activity.<sup>14</sup> In human myocardium, the AKAP18 $\delta$  orthologue, AKAP18 $\gamma$ , similarly complexes with PKA, PLN-SERCA2, and PDE3A1 (phosphodiesterase 3A1) to control Ser16-PLN phosphorylation and SR Ca<sup>2+</sup> reuptake.<sup>15</sup> In the present work, we show that AKAP18 $\delta$  also anchors CaMKII $\delta$  to PLN-SERCA2 and RYR, defining AKAP18 $\delta$  as the first CaMKII anchoring protein. We further identify 2 unique regions in AKAP18 $\delta$  that inversely regulate CaMKII $\delta$  activity, CaMKII $\delta$ -catalyzed phosphorylation of Thr17-PLN and Ser2814-RYR, and thus SERCA2 and RYR functional activities. This capability is enabled by one region of AKAP18 $\delta$ , which binds CaM and inhibits CaMKII activation, and a second region which lowers the Ca<sup>2+</sup> threshold for CaMKII $\delta$  activation and induces CaM trapping. Based on our results, we propose a model in which the 2 AKAP18 $\delta$  regions fine-tune the Ca<sup>2+</sup>-frequency-dependent activation of CaMKII $\delta$  at PLN-SERCA2 and RYR.

## METHODS

### Data Availability

The authors declare that all supporting data are available within the article and in its [Supplemental Material](#). Detailed methods are provided in the [Supplemental Material](#). The data that support the findings of this study and analytical tools are available from the corresponding author upon reasonable request.

### Statistics

All data sets with a small  $n$  ( $n < 8$ ) were tested for normal distribution using Kolmogorov-Smirnov, Shapiro-Wilk, or D'Agostino & Pearson normality test (GraphPad Prism 8.0.1 or 9.1.0). Differences between groups with normally distributed data were analyzed using ordinary 1-way ANOVA with Dunnett, Holm-Sidak, or Tukey multiple comparisons test, or unpaired  $t$  test for simple 2-group comparison. Non-normal distributions were examined by Wilcoxon matched-pairs signed-rank test, Mann-Whitney test, or Kruskal-Wallis with Dunn's multiple comparisons test. When multiple measures were drawn from individual animals, nested  $t$  test, nested 1-way ANOVA with Tukey or Dunnett multiple comparisons test or the linear mixed effect model from the R nlme package (<https://CRAN.R-project.org/package=nlme>) with Tukey post hoc correction was used. Only within-test corrections were made.  $P < 0.05$  were considered statistically significant. Outliers were removed using the ROUT method ( $Q = 1\%$ ) (GraphPad Prism) (Figure 6A, [Figure S3B and S3C](#) and [Figure S6A and S6B](#)). Power analysis was performed a priori to determine anticipated optimal sample size and number of adenoassociated virus-injected animals. All experiments were performed in a randomized manner, and data analysis was performed blinded using name and allocation concealment. Representative immunoblots were selected to represent the means of the quantified data. Representative images were selected by eye and based on good signal/noise ratios.

Other methods are given in details in the [Supplemental Material](#).

## RESULTS

### AKAP18 $\delta$ -Associated CaMKII $\delta$ Controls Thr17-PLN Phosphorylation

First, we tested whether CaMKII $\delta$  and AKAP18 $\delta$  interact at SERCA2-PLN. Immunoprecipitation analysis revealed co-precipitation of CaMKII $\delta$  and SERCA2 with AKAP18 $\delta$  in adult cardiomyocyte lysate (Figure 1A). High-resolution imaging of adult cardiomyocytes further demonstrated that AKAP18 $\delta$  and CaMKII $\delta$  (Figure 1B, blue, upper and lower respectively) co-localized with SERCA2 (red) at Z-line. AKAP18 $\delta$  also co-localized with SERCA2 at M-line where little CaMKII $\delta$  was observed, indicating a role for AKAP18 $\delta$  also within the sarcomere center (Figure 1B). Wheat germ agglutinin staining of t-tubules was used as marker for Z-lines, since these structures co-localize with  $\alpha$ -actinin (Figure S1D). Secondary antibody controls and specificity of CaMKII $\delta$  and AKAP18 $\delta$  antibodies are shown in [Figure S1E through S1G](#).

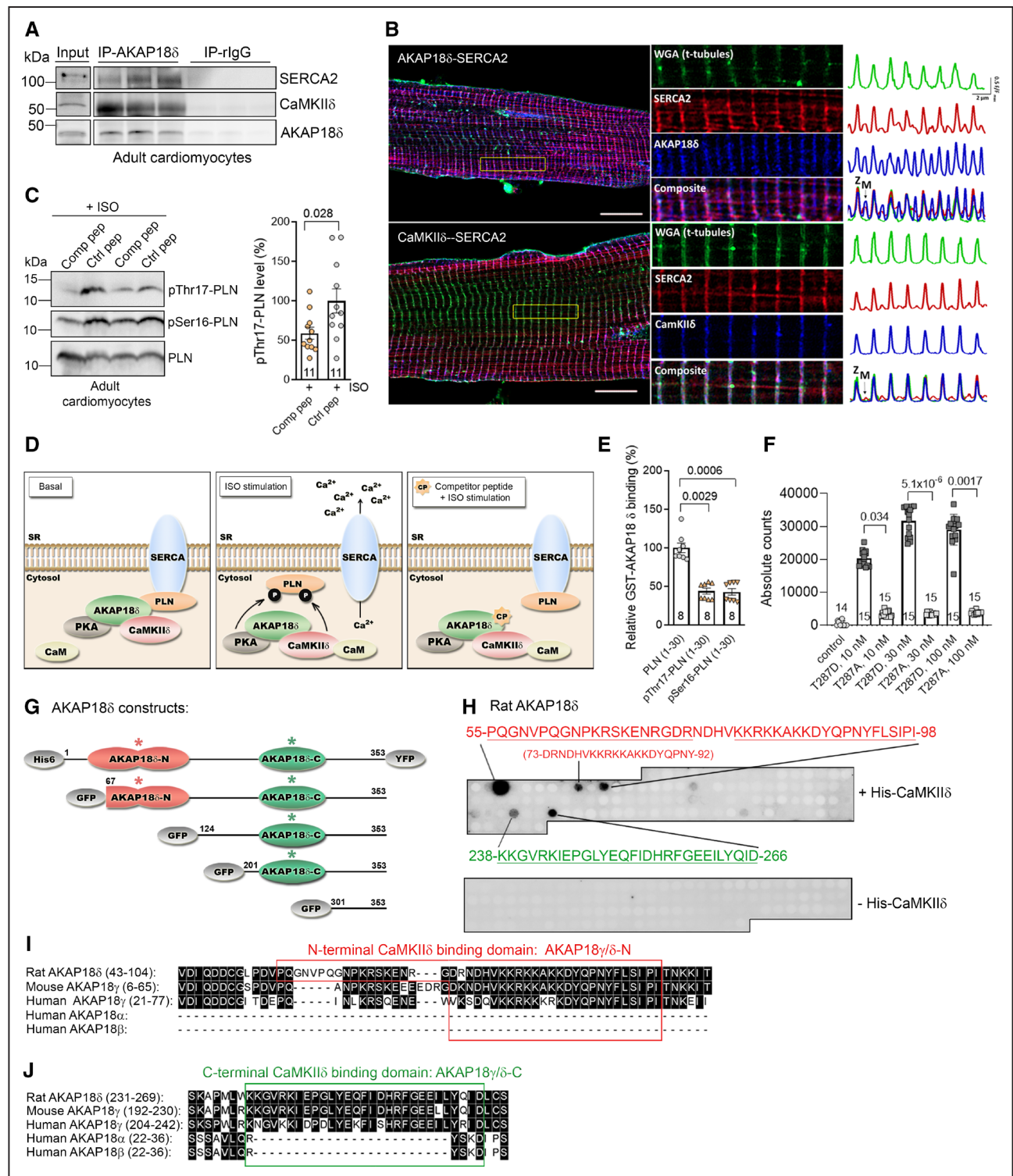


**Figure 1. AKAP18δ (A-kinase anchoring protein 18δ) anchors CaMKIIδ to the PLN (phospholamban)-sarcoplasmic reticulum (SR) Ca<sup>2+</sup>-ATPase 2 (SERCA2) complex and controls Thr17-PLN phosphorylation.**

**A**, Immunoprecipitation of CaMKIIδ-AKAP18δ from adult cardiomyocyte lysate detected by immunoblotting. Rabbit IgG was used as control. **B**, High-resolution imaging of SERCA2-AKAP18δ (upper) and SERCA2-CaMKIIδ (lower) in adult mouse cardiomyocytes using anti-SERCA2, anti-AKAP18δ, and anti-CaMKIIδ. Single images and corresponding traces are shown in middle and at right. Z/M-lines are indicated. Scale bars=10 μm. **C**, pThr17-PLN, pSer16-PLN, and PLN levels in ISO-stimulated adult cardiomyocytes pretreated with cell-permeant AKAP18δ-PLN competitor or control peptide. Normal distribution was confirmed by Shapiro-Wilk test. Significant differences were examined by the linear mixed effect model from the R nlme package with Tukey post hoc correction (n=11, 4 rats). **D**, Illustration of the AKAP18δ-PLN competitor experiment. Left: without ISO, PLN is dephosphorylated and inhibits SERCA2 activity. Middle: during ISO-stimulation, AKAP18δ-associated CaMKIIδ (and PKA) phosphorylates PLN, leading to SERCA2 activation and Ca<sup>2+</sup> uptake into SR. (Continued)

To analyze whether AKAP18 $\delta$ -associated CaMKII $\delta$  controls pThr17-PLN phosphorylation, AKAP18 $\delta$  was displaced from PLN using a cell-permeant AKAP18 $\delta$ -PLN competitor peptide.<sup>14</sup> Adult and neonatal cardiomyocytes treated with this peptide before isoproterenol stimulation exhibited reduced pThr17-PLN (and pSer16-PLN as previously reported<sup>14</sup>) compared with control (Figure 1C and Figure S1H, respectively), indicating that AKAP18 $\delta$ -associated CaMKII $\delta$  phosphorylates Thr17-PLN (illustrated in Figure 1D). The peptides showed no changes at basal level or cytotoxicity (Figure S1I and S1J, respectively). Using biotin-labeled PLN peptides, we found that Thr17 phosphorylation reduced GST (glutathione S-transferase)-AKAP18 $\delta$  binding (Figure 1E), closely paralleling reported effects of Ser16 phosphorylation.<sup>14</sup> Thus, Thr17 phosphorylation seems to provide an on/off mechanism for the AKAP18 $\delta$ -PLN interaction.

Taken together, the data strongly support that AKAP18 $\delta$  anchors CaMKII $\delta$  to PLN-SERCA2, and thereby controls CaMKII $\delta$ -mediated Thr17-PLN phosphorylation.

### CaMKII $\delta$ Binds Directly to 2 Unique Regions in AKAP18 $\delta$

The CaMKII $\delta$ -AKAP18 $\delta$  interaction was further investigated using AlphaScreen technology. Only recombinant CaMKII $\delta$ -T287D (mimicking active kinase)<sup>16</sup> and not CaMKII $\delta$ -T287A (mimicking inactive kinase) (mutated proteins are validated in Figure S1K and S1L) was found to bind to AKAP18 $\delta$  (Figure 1F), indicating that AKAP18 $\delta$  binds to autophosphorylated CaMKII $\delta$ .

To identify CaMKII $\delta$ -binding sites, AKAP18 $\delta$ -YFP variants (Figure 1G) were co-expressed with CaMKII $\delta$ -T287D. CaMKII $\delta$  precipitated all AKAP18 $\delta$  variants, except for GFP-AKAP18 $\delta$  (301-353) (Figure S1M), indicating that CaMKII $\delta$  binds between amino acids 201-301 (Figure 1G, green region). This region is located C-terminally from the PLN binding domain (amino acids 124-220<sup>14</sup>) and N-terminally from the PKA binding domain (amino acids 301-314<sup>13</sup>). In addition, AKAP18 $\delta$ -YFP and GFP-AKAP18 $\delta$  (67-353) precipitated more strongly with CaMKII $\delta$  compared with other AKAP18 $\delta$  variants, consistent with a second CaMKII $\delta$ -binding site toward the N-terminus of AKAP18 $\delta$  (Figure 1G, red).

To more precisely identify CaMKII $\delta$  binding, rat AKAP18 $\delta$  was spot-synthesized as 20-mer overlapping peptides on membranes and incubated with active His-CaMKII $\delta$ . Immunoblotting identified CaMKII $\delta$  binding to 2 regions; amino acids 55-98 (AKAP18 $\delta$ -N, in red) and 238-266 (AKAP18 $\delta$ -C, in green) (Figure 1H) and 2 homologous regions in human AKAP18 $\gamma$  (Figure S1N). CaMKII $\delta$ -T287D (coated in wells) binding was confirmed by an ELISA-based method using biotinylated peptides spanning the 2 AKAP18 $\delta$  regions (Figure S1O and S1P). Sequence alignments showed that the 2 CaMKII $\delta$ -binding regions were only present in AKAP18 $\delta$  and AKAP18 $\gamma$  and not in the shorter AKAP18 $\alpha$  and AKAP18 $\beta$  isoforms<sup>13</sup> (Figure 1I and 1J).

### AKAP18 $\delta$ Binds CaMKII $\delta$ Through Multiple Sites

We next sought to define AKAP18 $\delta$  binding in CaMKII $\delta$ <sub>C/27</sub>, which is largely cytoplasmic and regulates ECC. CaMKII $\delta$  was spot-synthesized as 20-mer overlapping peptides on membranes, which were overlaid with GST-AKAP18 $\delta$  (Figure 2A). AKAP18 $\delta$  bound to the ATP-binding region<sup>7</sup> (amino acids 19-68), S-site (amino acids 130-164) and T-site regions (amino acids 241-269) and a sequence within the autoregulatory domain (amino acids 280-317)<sup>7</sup> (Figure 2A, GST only as negative control is shown in Figure S2A, bottom). Notably, the S- and T-site regions within the catalytic domain have not been clearly defined but are reported to contain at least residues Glu97 (S-site), Glu140 (S-site), Ile206 (T-site), and Trp238 (T-site)<sup>19</sup> (Figure 2A, boxed regions in upper panel). Consistent with the above results, a biotinylated peptide covering the N-terminal region of AKAP18 $\delta$  (55-98; Figure S2B) showed an almost identical CaMKII $\delta$  binding pattern as GST-AKAP18 $\delta$ .

CaMKII $\delta$  binding of biotin-ahx-AKAP18 $\delta$ -C was too weak or dynamic to be detected by peptide arrays. However, overlaying a larger recombinant GST-AKAP18 $\delta$ -C fragment (amino acids 201-301), revealed a binding site residing centrally within the T-site region (amino acids 205-233) (Figure 2B). This binding site was not detected using GST-AKAP18 $\delta$  full length protein, suggesting that GST-AKAP18 $\delta$  (201-301) exhibits differential folding. These data are consistent with AKAP18 $\delta$ -C

**Figure 1 Continued.** Right: in the presence of the cell-permeant AKAP18 $\delta$ -PLN competitor peptide (CP),<sup>14</sup> AKAP18 $\delta$  displaces from PLN-SERCA2. AKAP18 $\delta$ -associated CaMKII $\delta$  is no longer able to phosphorylate PLN. Both AKAP18 $\delta$ <sup>76</sup> and PLN locate to membrane, but this is not shown for simplicity. **E**, Analyses of biotin-ahx-PLN (1-30), biotin-ahx-pSer16-PLN (1-30), and biotin-ahx-pThr17-PLN (1-30) binding to GST-AKAP18 $\delta$  (coated in wells) by an ELISA-based assay. Binding was detected with a biotin-HRP conjugated antibody and incubation with Ultra TMB. Significant differences were examined by Kruskal-Wallis with Dunn's multiple comparisons test (n=8). **F**, Analysis of AKAP18 $\delta$ -CaMKII $\delta$  interaction by AlphaScreen™. GST-AKAP18 $\delta$  was incubated with increasing concentrations of recombinant CaMKII $\delta$ -T287D or CaMKII $\delta$ -T287A. Significant differences were examined by Kruskal-Wallis with Dunn multiple comparisons test (n=14–15). **G**, The 2 CaMKII $\delta$  binding regions in AKAP18 $\delta$  are illustrated in red and green. **H**, Residues important for CaMKII $\delta$  binding were identified by overlaying 20-mer overlapping AKAP18 $\delta$  peptides spot-synthesized on membranes with active His-CaMKII $\delta$  and immunoblotting. Immunoblotting without His-CaMKII $\delta$  was used as control (lower). Underlined sequences were synthesized as soluble peptides for further experiments. **I** and **J**, The 2 CaMKII $\delta$ -binding regions (red and green) are indicated in the alignment of rat AKAP18 $\delta$ , human and mouse AKAP18 $\gamma$ , and the smaller AKAP18 $\alpha$  and AKAP18 $\beta$ . Black boxes indicate identical amino acids (DNA Star).

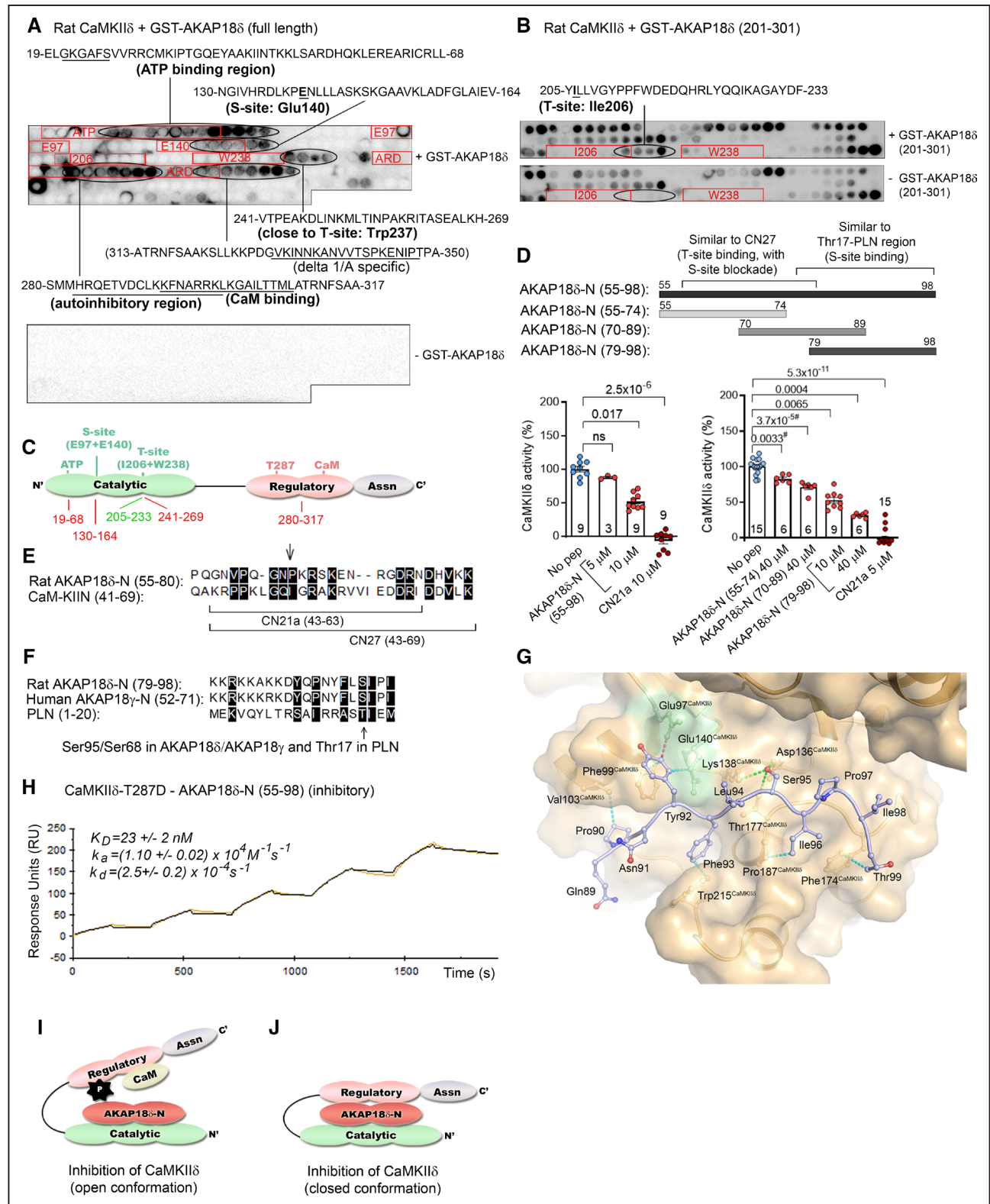


**Figure 2. AKAP18δ (A-kinase anchoring protein 18δ) binds CaMKIIδ through multiple sites and inhibits CaMKIIδ through sequences similar to the natural CaMKII inhibitor protein and Thr17-PLN (phospholamban) region.** AKAP18δ binding was identified by overlaying 20-mer overlapping CaMKIIδ peptides with (A) GST-AKAP18δ or (B) GST-AKAP18δ (201-301) and immunoblotting with anti-GST-HRP. Immunoblotting without recombinant protein (lower) or GST (Figure S2A, lower) was used as control. Peptides containing ATP-binding region<sup>7</sup> (ATP-binding motif underlined), S-site (E97 and E140-containing sequences), T-site (I206 and W238-containing sequences) or autoregulatory domain (ARD) are boxed. Stretches of spots that were not apparent in negative controls were regarded as potential-binding sites. Sequences for spots with strongest signal are given. Autoinhibitory region and (Continued)

and AKAP18 $\delta$ -N binding to distinct T-site sequences. ELISA-based experiments confirmed AKAP18 $\delta$  binding to the autoregulatory domain, ATP binding region, S-site and 2 T-site regions of CaMKII $\delta$  (Figure S2C through S2E), supporting the interpretation of the overlay data. The 5 AKAP18 $\delta$  binding sites in CaMKII $\delta_{C/2}$  are indicated in Figure 2C (19-68, 130-164, 205-233, 241-269, and 280-317, inhibitory ones in red and activating in green). The fact that AKAP18 $\delta$ -N binds to several different regions in these critical CaMKII domains may serve to stabilize (or rigidify) CaMKII in the closed inactivated state. Multiple CaMKII-binding sites have also been identified in other proteins,<sup>17,18,20</sup> for example, densin, which binds to several T-site sequences.<sup>18</sup>

### AKAP18 $\delta$ -N Inhibits CaMKII $\delta$ Through Sequences Similar to the Natural CaMKII Inhibitor Protein and Thr17-PLN Region

AKAP18 $\delta$ -N (55-98) interacted only with activated CaMKII $\delta$  (Figure S2F). The effect of AKAP18 $\delta$ -N on CaMKII $\delta$  activity was analyzed in an in vitro kinase assay. AKAP18 $\delta$ -N (55-98) reduced CaMKII $\delta$ -catalyzed phosphorylation of syntide (a CaMKII substrate) by 50% under high [Ca<sup>2+</sup>] and [CaM], conditions that should maximally activate CaMKII (Figure 2D, left panel). Closer examination showed that amino acids 55-74 were less inhibitory (right panel). Bioinformatics revealed that this sequence exhibited similarities to CN27, a natural CaMKII inhibitory peptide<sup>21</sup> (Figure 2E). In a crystal structure of CaMKII, a shorter variant of CN27 (CN21a in Figure 2E) has been shown to bind to the T-site, while being sufficiently long to prevent access for substrate binding to the adjacent S-site.<sup>21</sup> In an ELISA-based assay, CN27 outcompeted the AKAP18 $\delta$ -N (55-74)-CaMKII $\delta$  interaction, indicating that CN27 and AKAP18 $\delta$ -N (55-74) may bind to the same site in CaMKII $\delta$  (Figure S2G). In addition, AKAP18 $\delta$ -N (55-74) contains a proline (Pro64) in its central region (Figure 2E, arrow); a feature also reported for the inhibitory T-site binding sequence in densin,<sup>18</sup> which might explain its weaker effect on CaMKII $\delta$  activity.

CaMKII $\delta$  binding of the more inhibitory amino acids 79-98 of AKAP18 $\delta$  (Figure 2D) were not outcompeted by CN27 (Figure S2H). Bioinformatics revealed that these amino acids rather showed some sequence similarity to the Thr17-PLN region, with Ser95<sup>AKAP18 $\delta$</sup>  corresponding to Thr17<sup>PLN</sup> (Figure 2F). Modeled placement of AKAP18 $\delta$  (89-99) into the peptide binding groove of CaMKII $\delta$  centered on Ser95 in AKAP18 $\delta$  (Figure 2G) and suggested several favorable interactions between CaMKII $\delta$  and AKAP18 $\delta$ . Hydrophobic interactions between Pro90-Val103<sup>CaMKII $\delta$</sup> , Tyr92-Lys138<sup>CaMKII $\delta$</sup> , Phe93-Trp215<sup>CaMKII $\delta$</sup> , Ile96-Pro187<sup>CaMKII $\delta$</sup> , and Thr99-Phe174<sup>CaMKII $\delta$</sup>  were suggested (cyan dashed lines). The model indicated that Ser95 could interact with both Asp136<sup>CaMKII $\delta$</sup> , Lys138<sup>CaMKII $\delta$</sup>  and Thr177<sup>CaMKII $\delta$</sup>  (green dashed lines) via hydrogen bonds. A possible unfavorable repulsive interaction between Tyr92 and Glu97<sup>CaMKII $\delta$</sup>  was also indicated (red dashed line). Model predictions were validated by mutating key residues in AKAP18 $\delta$ , and subsequent ELISA analysis (Figure S2I, see legend for detailed description).

Kinetics of AKAP18 $\delta$ -N (55-98) binding to CaMKII $\delta$  were analyzed by surface plasmon resonance (SPR). A range of concentrations of recombinant CaMKII $\delta$ -T287D (47.6–500 nmol/L) was injected over immobilized biotin-AKAP18 $\delta$ -N on a streptavidin affinity chip and analyzed by fitting with a 1:1 interaction model (Langmuir). The dissociation equilibrium constant ( $K_D$ ) was  $23 \pm 2$  nM, with an association rate constant ( $k_a$ ) =  $(1.10 \pm 0.02) \times 10^4$  M<sup>-1</sup> s<sup>-1</sup> and a dissociation rate constant ( $k_d$ ) =  $(2.5 \pm 0.2) \times 10^{-4}$  s<sup>-1</sup> (Figure 2H). These findings indicate a strong CaMKII $\delta$ -T287D interaction with AKAP18 $\delta$ -N with medium association and dissociation rates. We also performed SPR analyses of AKAP18 $\delta$ -N (55-74) and AKAP18 $\delta$ -N (79-98). The inhibitory AKAP18 $\delta$ -N (79-98) bound strongly to CaMKII $\delta$ -T287D with similar SPR values as identified above (Figure S2J). AKAP18 $\delta$ -N (55-74), which was less inhibitory and contained a proline in its central region, bound more weakly and exhibited higher association and dissociation rate constants (faster on/off) (Figure S2K).

Taken together, our data indicate that AKAP18 $\delta$ -N (55-98) is a potent inhibitor of the open CaMKII $\delta$

**Figure 2 Continued.** CaM-binding site are underlined.<sup>7</sup> The CaMKII $\delta$ 1/A-specific sequence is only present in neonatal mouse hearts.<sup>77</sup> Amino acids 205-233 (upper in **B**) was regarded as potential-binding site, since it was absent in negative control (lower). **C**, The 5 AKAP18 $\delta$ -binding regions identified by peptide arrays (in **A** and **B**) are indicated in CaMKII $\delta$ 2/C (inhibitory ones in red and activating in green). **D**, Effect of different AKAP18 $\delta$ -N sequences on CaMKII $\delta$ -T287D activity (<sup>32</sup>P incorporation into syntide). CN21a derived from natural CaMKII inhibitor protein (CaM-KIIN)<sup>21</sup> was used as control. Significant differences were examined by Kruskal-Wallis with Dunn's multiple comparisons test (n=3-9 in left, n=6-15 in right). #Significant differences were detected by Mann-Whitney *U* test. Upper panel illustrates the different AKAP18 $\delta$ -N peptides. **E**, Alignment of rat AKAP18 $\delta$  (55-80) with the natural CaMKII inhibitor protein (amino acids 41-69). CN27 and CN21a are indicated.<sup>21</sup> Arrow denotes a proline in AKAP18 $\delta$ . **F**, Alignment of rat AKAP18 $\delta$  (79-98) and human AKAP18 $\gamma$  (52-71) with PLN (1-20). Arrow indicates Ser68/Ser95 in AKAP18 $\gamma$ /AKAP18 $\delta$  and Thr17 in PLN. Black boxes indicate identical or functionally similar amino acids (DNA Star). **G**, Structural model of the AKAP18 $\delta$  (89-QPNYFLSIPIT-99) binding to CaMKII $\delta$  centered at Ser95 (corresponds to Thr17 in PLN). AKAP18 $\delta$  is shown as a ball-and-stick model, while CaMKII $\delta$  peptide backbone is shown as a cartoon with central residues as a ball-and-stick motif. The negatively charged patch around S-site residues Glu97 and Glu140 is colored light green. Rest of the transparent CaMKII $\delta$  surface is shown in yellow. **H**, SPR analysis of immobilized biotin-ahx-AKAP18 $\delta$  (55-98) on an SA chip and recombinant CaMKII $\delta$ -T287D injected at a range of concentrations (47.6–500 nmol/L) (n=3). **I** and **J**, Illustration of CaMKII $\delta$  inhibition by AKAP18 $\delta$ -N. AKAP18 $\delta$ -N (red) binds to catalytic region (light green) and inhibits CaMKII $\delta$  in both an (**I**) open and (**J**) closed conformation after pThr287 dephosphorylation and CaM dissociation.

with strong affinity. Inhibition is effected by sequences with similarities to CN27 derived from natural CaMKII inhibitor protein (T-site binding, with associated S-site blockade) and Thr17-PLN region (S-site binding) (summarized in Figure 2D, upper panel). CaMKIIδ inhibition by AKAP18δ-N is illustrated in Figure 2I (open conformation). Since AKAP18δ-N also bound to the autoregulatory domain, it is likely that AKAP18δ-N also continues to bind and inhibit CaMKIIδ after pThr287 dephosphorylation and CaM dissociation (Figure 2J, closed conformation).

### AKAP18δ-N Reduces pThr17-PLN and Inhibits SR Ca<sup>2+</sup> Reuptake

Analyses performed using biotin-ahx-PLN (1-30) as a substrate showed that AKAP18δ-N reduced CaMKIIδ-T287D-catalyzed phosphorylation of Thr17 in PLN (Figure 3A, full immunoblots in Figure S3A). We further examined whether AKAP18δ-N also reduced Thr17-PLN phosphorylation in cardiomyocytes. Compared with the scrambled control peptide, cell-permeant AKAP18δ-N (55-74) reduced the pThr17-PLN level in both isoproterenol treated (15 minutes) adult (Figure 3B) and neonatal cardiomyocytes (Figure S3B), whereas pSer16, which is a PKA substrate, was hardly affected. Neither AKAP18δ-N (55-74) nor control peptide showed any changes at basal level or cytotoxicity (Figure S3C and S3D, respectively).

Effects of AKAP18δ-N on Ca<sup>2+</sup> fluxes in adult cardiomyocytes were also investigated. Rat adult cardiomyocytes were treated with the cell-permeant version of AKAP18δ-N (55-74) or a scrambled control peptide, with or without isoproterenol stimulation. Cell-permeant TAT-AKAP18δ-N (55-74) treatment prolonged decay time of Ca<sup>2+</sup> transients at 4 Hz (Figure 3C, representative tracings are shown in Figure S3E), where Thr17-PLN phosphorylation is increased<sup>40</sup> and SERCA2 plays a proportionally larger role in controlling Ca<sup>2+</sup> removal from the cytosol.<sup>41</sup> In the presence of isoproterenol, which augments SERCA2 activity via PLN phosphorylation, TAT-AKAP18δ-N (55-74) continued to slow Ca<sup>2+</sup> transient decay at high stimulation frequencies (4 and 6 Hz) (Figure 3D, representative tracings are shown in Figure S3F). Compared with the scrambled control peptide, AKAP18δ-N (79-98) also reduced SERCA2 Ca<sup>2+</sup> reuptake rate in isolated mouse cardiac SR vesicles (Figure 3E). These findings are consistent with reduction of pThr17-PLN levels by AKAP18δ-N (Figure 3A and 3B).

Finally, compared with control mice, adult mice injected with adenoassociated virus encoding AKAP18δ-N (55-74) exhibited reduced pThr17-PLN levels after isoproterenol stimulation, suggesting that AKAP18δ-N (55-74) also inhibits CaMKIIδ-catalyzed phosphorylation of Thr17 in PLN in vivo (Figure 3F, upper panel). No

effect of adenoassociated virus-AKAP18δ-N (55-74) on pSer16-PLN was observed (Figure 3F, middle panel).

### Calcified CaM Binds to AKAP18δ-N in Competition With CaMKIIδ

Rat AKAP18δ-N and human AKAP18γ-N contain stretches of alternating hydrophobic and basic residues, including valine (V), lysine (K), arginine (R), phenylalanine (F), and proline (P), which are characteristic for CaM-binding motifs.<sup>23</sup> Closer inspection revealed that both AKAPs showed sequence similarities to the CaM-binding motif in AKAP79<sup>24</sup> (Figure 4A) and CaMKIIδ (Figure S4A). We therefore analyzed whether AKAP18δ-N also bound calcified CaM. Immunoblotting demonstrated that the inhibitory AKAP18δ-N (79-98) peptide, the corresponding sequence in human AKAP18γ-N (52-71) and GFP-AKAP18δ (67-353) precipitated with CaM-agarose in the presence of Ca<sup>2+</sup> (Figure S4B through S4D, respectively). CaM binding to AKAP18δ-N (79-98) was also confirmed in an ELISA-based assay where CaM-coated wells were incubated with biotinylated AKAP18δ-N (79-98) or the scrambled control (Figure 4B). Interestingly, in further experiments, the presence of CaM attenuated both the inhibitory AKAP18δ-N (79-98)-CaMKIIδ-T287D (Figure 4C) and AKAP18δ-N (79-98)-CaMKIIδ (1-282) (Figure 4D) interactions. Since CaMKIIδ (1-282) lacks the CaM-binding site, this finding indicates that CaM also outcompetes AKAP18δ-N (79-98) binding to the CaMKIIδ catalytic site.

Kinetics of the CaM-AKAP18δ-N (79-98) interaction were analyzed by SPR. In the presence of 1 mM Ca<sup>2+</sup>, the dissociation equilibrium constant ( $K_d$ ) was  $4.7 \pm 0.7 \mu\text{M}$ , with an association rate constant ( $k_a$ ) =  $(1.3 \pm 0.3) \times 10^2 \text{ M}^{-1} \text{ s}^{-1}$  and a dissociation rate constant ( $k_d$ ) =  $(5.3 \pm 0.3) \times 10^{-4} \text{ s}^{-1}$  (Figure 4E). These findings indicate that the CaM-AKAP18δ-N (79-98) interaction is quite slow and weak.

In summary, our data indicate that calcified CaM binds directly to AKAP18δ-N and outcompetes the inhibitory AKAP18δ-N-CaMKIIδ interaction (illustrated in Figure 4F). By this mechanism, rising Ca<sup>2+</sup> levels, and resulting calcification of CaM, relieve the inhibition of CaMKII.

### AKAP18δ-C Is Homologous to the Neuronal CaMKIIα Activator N2B-s and Lowers the Ca<sup>2+</sup> Threshold for CaMKIIδ Activation

As shown in Figure 1J, both AKAP18δ and AKAP18γ contain a second CaMKIIδ interaction site positioned toward the C-terminus. Bioinformatics revealed that this region showed sequence similarity to the N2B-s sequence derived from the neuronal N-methyl-D-aspartate receptor NR2B subunit (Figure 5A). N2B-s is homologous to the Thr286 autoinhibitory region in CaMKIIα and linked to autonomous CaMKIIα activation in brain via T-site binding.<sup>17,25,26</sup> As demonstrated



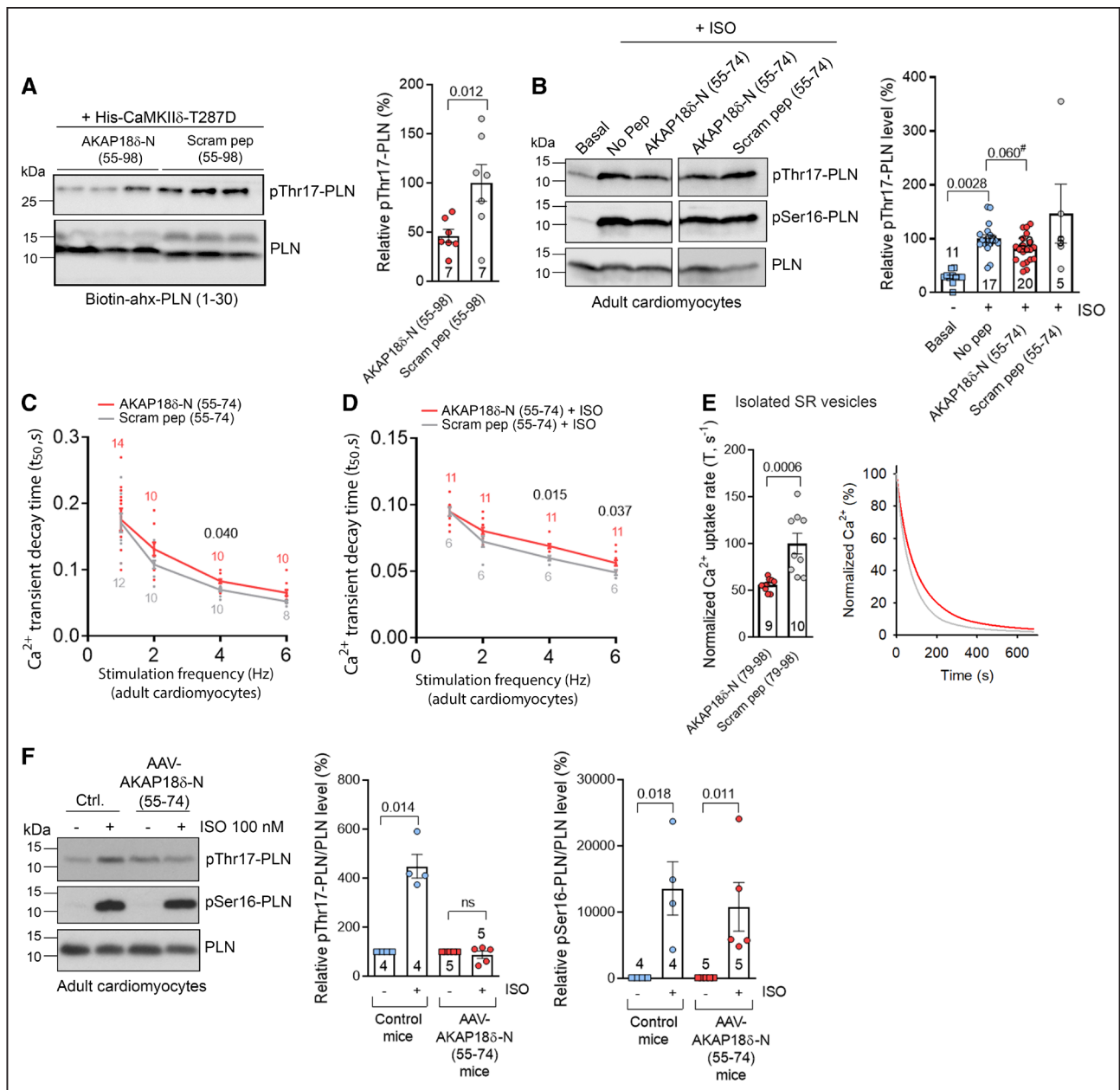


**Figure 3. AKAP18 $\delta$  (A-kinase anchoring protein 18 $\delta$ )-N reduces pThr17-PLN (phospholamban) and inhibits Ca<sup>2+</sup> reuptake into sarcoplasmic reticulum (SR).**

**A**, CaMKII $\delta$  phosphorylation of biotin-ahx-PLN (1-30), in the presence of AKAP18 $\delta$ -N (55-98) or a scrambled control peptide. Phosphorylated Thr17-PLN was observed at 25 kDa consistent with induced oligomerization<sup>78</sup> (Figure S3A, complete immunoblots). Normal distribution was confirmed by Shapiro-Wilk test. Significant differences were examined by unpaired *t* test ( $n=7$ ). **B**, Adult cardiomyocytes were treated with TAT-AKAP18 $\delta$ -N (55-74) or the scrambled control for 45 min before ISO-stimulation (15 min) and immunoblotted with pThr17-PLN, pSer16-PLN, and PLN antibodies. pThr17-PLN was quantified against PLN or GAPDH. Normal distribution was confirmed by Shapiro-Wilk test (not tested for scram pep with  $n<6$ ). Significant differences were examined by nested 1-way ANOVA with Tukey's multiple comparisons test ( $n=5-20$ , 2-6 rats). #Significant differences were examined by nested *t* test. The effect of TAT-AKAP18 $\delta$ -N (55-74) on decay time of Ca<sup>2+</sup> transients at different stimulation frequencies of adult cardiomyocytes in the (**C**) absence or (**D**) presence of ISO. Scrambled TAT-AKAP18 $\delta$ -N (55-74) peptide was used as control. Normal distribution was confirmed by Shapiro-Wilk test (in **C**) and Kolmogorov-Smirnov or D'Agostino and Pearson test (in **D**), except for the scrambled peptide at 1 Hz. Significant difference was examined by nested *t* test,  $n=8-14$  in **C** (2-4 rats) and  $n=6-11$  in **D** (3-4 rats). Representative Ca<sup>2+</sup> tracings are shown in Figure S3E and S3F. **E**, The effect of TAT-AKAP18 $\delta$ -N (79-98) or a scrambled control on SERCA2 Ca<sup>2+</sup> reuptake rate in isolated mouse SR vesicles (left ventricle crude homogenate). Normal distribution was confirmed by D'Agostino and Pearson test. Significant differences were examined by unpaired *t* test,  $n=9-10$ . **F**, Levels of pThr17-PLN, pSer16-PLN, and PLN in adult cardiomyocytes isolated from control (WT) and AAV-AKAP18 $\delta$ -N (79-98) mice, treated with or without ISO. Significant differences were examined by Kruskal-Wallis with Dunn multiple comparisons test ( $n=4-5$ , 3-4 mice in each group).

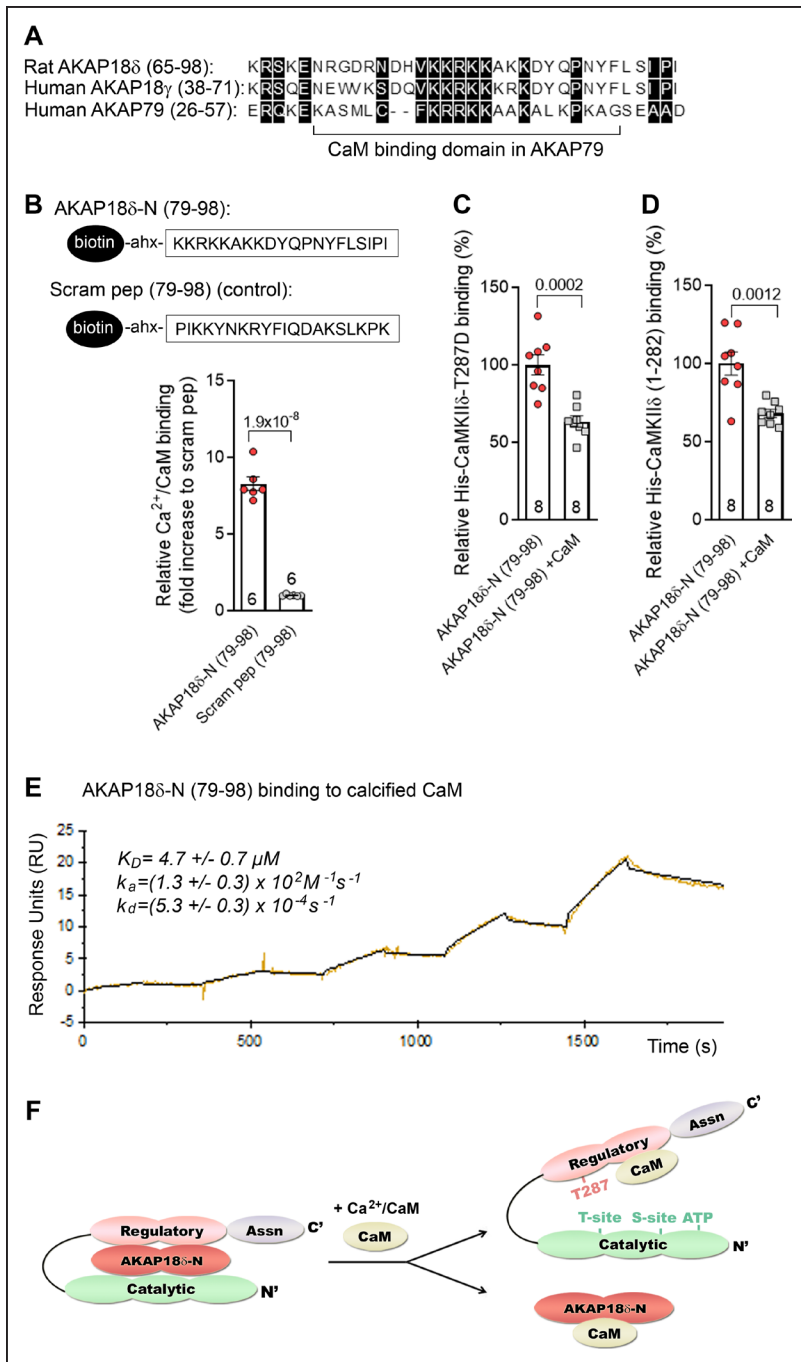


**Figure 4. Calcified CaM (calmodulin) binds to AKAP18δ (A-kinase anchoring protein 18δ)-N and outcompetes the inhibitory AKAP18δ-N-CaMKIIδ interaction.**

**A**, Alignment of rat AKAP18δ-N (65-98) and human AKAP18γ (38-71) with the CaM-binding domain in AKAP79.<sup>24</sup> Black boxes indicate identical or functional similar amino acids (DNA Star). **B**, Binding of biotin-ahx-AKAP18δ-N (79-98) and a scrambled control to Ca<sup>2+</sup>/CaM (coated in wells) analyzed by an ELISA-based method. Normal distribution was confirmed by Kolmogorov-Smirnov test. Significant differences were examined by unpaired *t* test (n=6). Biotinylated AKAP18δ-N (79-98) peptide was incubated with or without CaM in wells coated with recombinant **(C)** CaMKIIδ-T287D or **(D)** CaMKIIδ (1-282). Binding was detected with anti-biotin-HRP. Normal distribution was confirmed by Shapiro-Wilk test (**C** and **D**). Significant differences were examined by unpaired *t* test (n=8 in **C** and **D**). **E**, SPR analysis of immobilized biotin-ahx-AKAP18δ (79-98) and recombinant CaM injected (952.6–10 000 nmol/L) (n=3). **F**, CaM (beige) outcompetes the inhibitory AKAP18δ-N-CaMKIIδ interaction upon binding to the CaMKIIδ regulatory region (pink) and AKAP18δ-N (red).

in Figure 2B, AKAP18δ-C also bound to T site (amino acids 205-233).

In similarity to effects of N2B-s, we observed that AKAP18δ-C increased substrate phosphorylation by CaMKIIδ-T287A in an in vitro kinase assay where CaM was omitted (Figure 5B). This finding suggests that AKAP18δ-C augments CaMKIIδ activity independently of Thr287 autophosphorylation and CaM binding. Consistently, cell-permeant TAT-AKAP18δ-C also increased Camui activity,<sup>27</sup> a fluorescence resonance energy transfer-based CaMKII activation state sensor, transduced into adult rabbit ventricular myocytes (Figure 5C). As CaMKII

requires relatively high intracellular Ca<sup>2+</sup> to achieve activation, we hypothesized that AKAP18δ-C was able to decrease the Ca<sup>2+</sup> threshold for CaMKIIδ activation. Indeed, at 0.5 μM free Ca<sup>2+</sup>, which does not fully activate CaMKIIδ-T287A to phosphorylate Thr17-PLN, further increased Thr17-PLN phosphorylation in the presence of either AKAP18δ-C (tendency) or the N2B-s positive control peptide (Figure 5D and 5E, respectively, complete immunoblots in Figure S5A and S5B). These observations suggest that AKAP18δ-C is able to potentiate CaMKIIδ by keeping the inhibitory gate open as a wedge, thereby sensitizing CaMKII to Ca<sup>2+</sup>-dependent activation.

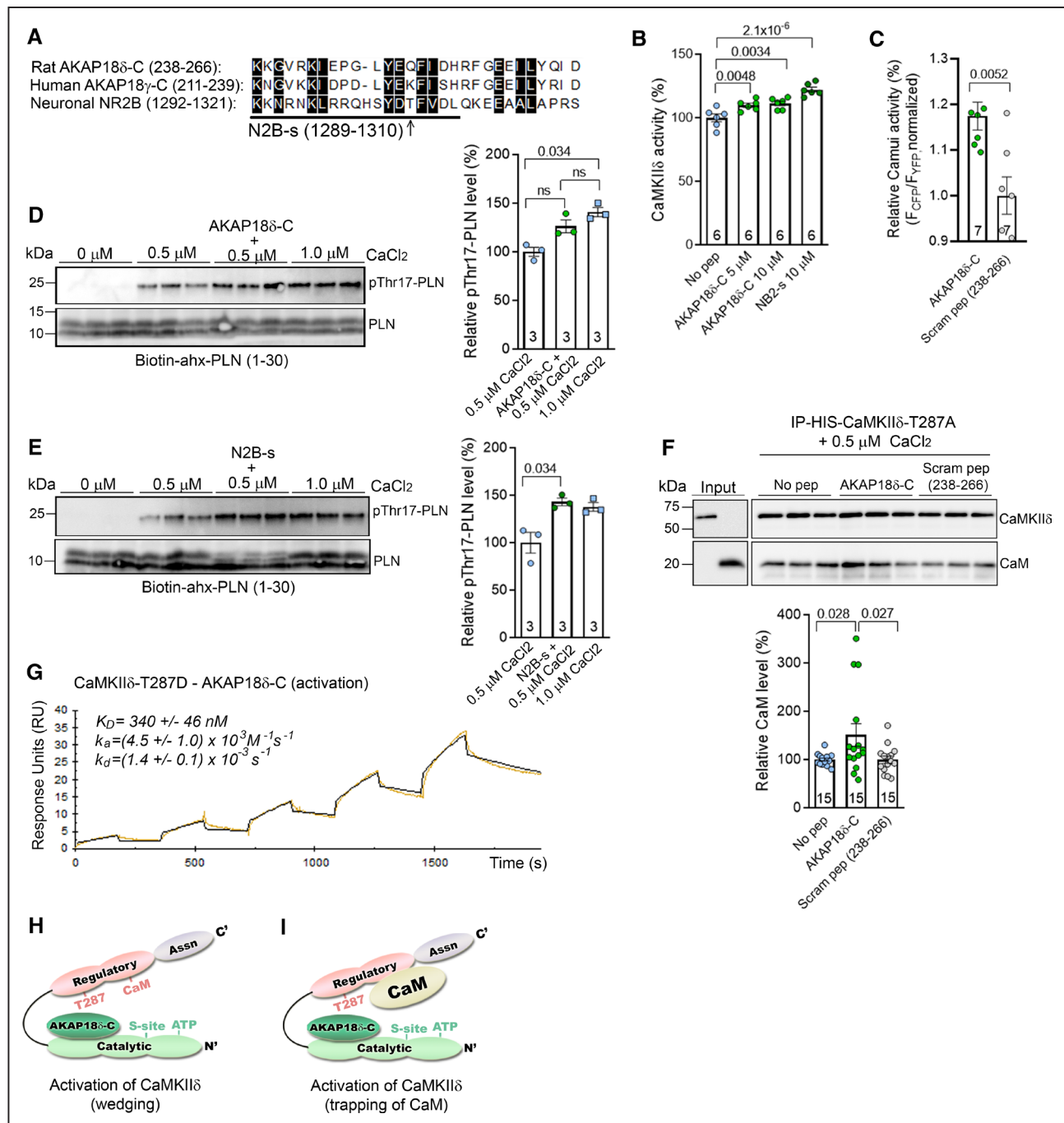


**Figure 5. AKAP18 $\delta$  (A-kinase anchoring protein 18 $\delta$ )-C is homologous to the neuronal CaMKII $\alpha$  activator N2B-s and lowers the Ca<sup>2+</sup> threshold for CaMKII $\delta$  activation.**

**A**, Alignment of AKAP18 $\delta$ -C (238-266) and AKAP18 $\gamma$ -C (211-239) with CaMKII $\alpha$  binding site in neuronal NMDA receptor NR2B subunit (amino acids 1289-1321).<sup>17</sup> N2B-s (1292-1310) is underlined. Arrow denotes CaMKII $\alpha$  phosphorylation site in NR2B (Thr1306). Black boxes indicate identical or functionally similar amino acids. **B**, Effect of AKAP18 $\delta$ -C on CaMKII $\delta$ -T287A activity analyzed in a CaMKII kinase assay in the absence of CaM (<sup>32</sup>P incorporation into syntide). N2B-s<sup>17</sup> and CN21a<sup>21</sup> were used as controls. Normal distribution was confirmed by Shapiro-Wilk test. Significant differences were examined by ordinary 1-way ANOVA with Holm-Sidak multiple comparisons test (n=6). **C**, Effect of TAT-AKAP18 $\delta$ -C on a Camui FRET-based biosensor,<sup>27</sup> transduced into adult rabbit ventricular myocytes. Normal distribution was confirmed by Shapiro-Wilk test. Significant differences were examined by unpaired *t* test (n=7). Immunoblot analysis of CaMKII $\delta$ -catalyzed phosphorylation of Thr17-PLN (phospholamban) at 0.5  $\mu$ M CaCl<sub>2</sub> with or without the presence of **(D)** AKAP18 $\delta$ -C or **(E)** N2B-s. Significant differences were examined by Kruskal-Wallis with Dunn's multiple comparisons test **(D and E)**. **F**, Immunoblot analyses of immunoprecipitations of CaM with CaMKII $\delta$ -T287A in the absence or presence of AKAP18 $\delta$ -C (n=15). Normal distribution was confirmed by D'Agostino & Pearson test, and significant differences were examined by ordinary 1-way ANOVA with Dunnett multiple comparisons test. **G**, SPR analysis of immobilized biotin-ahx-AKAP18 $\delta$ -C and recombinant CaMKII $\delta$ -T287D injected (95.2–1000 nmol/L) (n=3). **H and I**, AKAP18 $\delta$ -C (dark green) binds to catalytic region of CaMKII $\delta$  (light green) and activates CaMKII $\delta$  by **(H)** lowering the Ca<sup>2+</sup> threshold for activation by keeping the inhibitory gate open and **(I)** trapping CaM (beige) within the kinase.

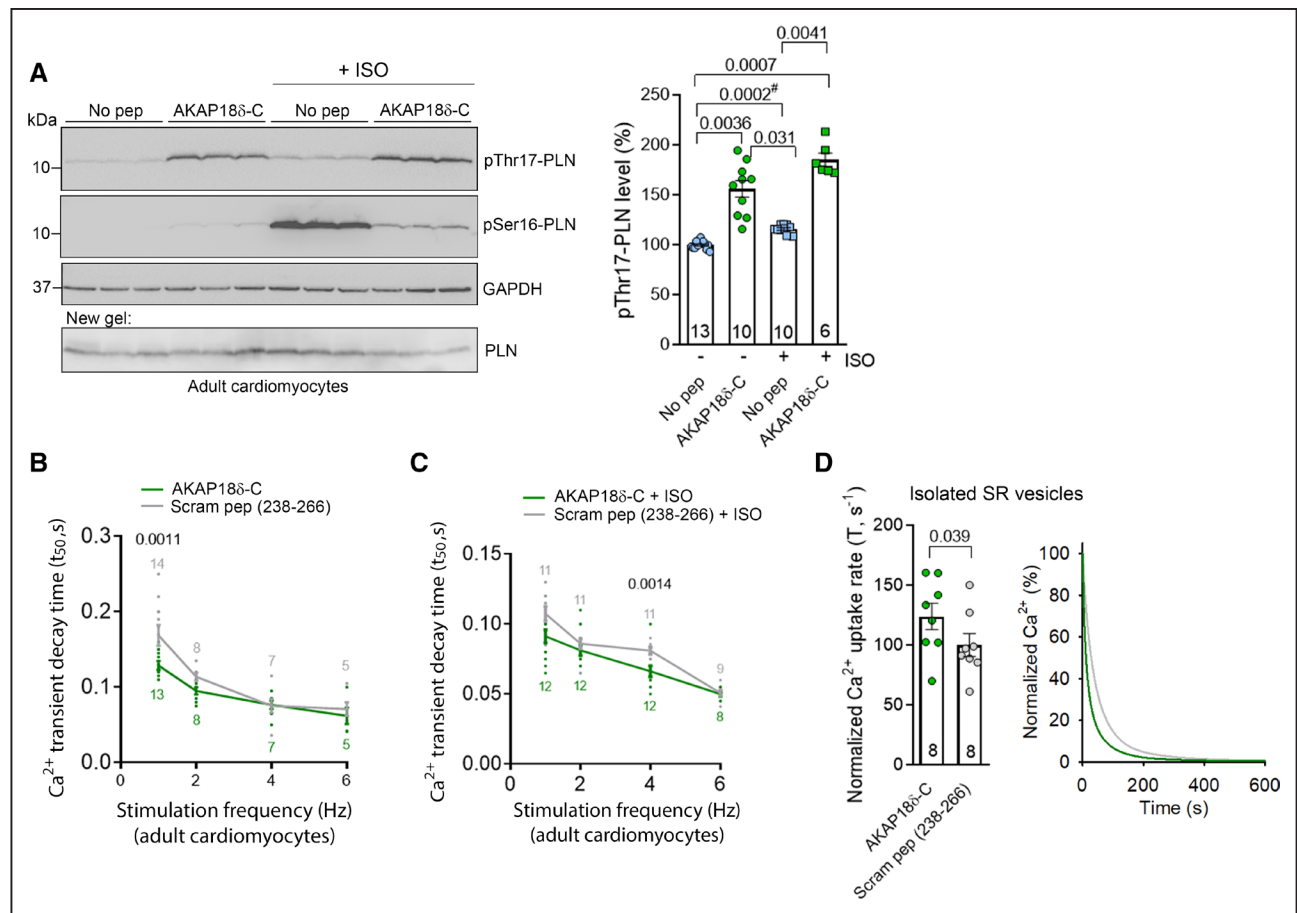


**Figure 6. AKAP18 $\delta$  (A-kinase anchoring protein 18 $\delta$ )-C increases pThr17-PLN (phospholamban) and facilitates faster Ca<sup>2+</sup> reuptake into sarcoplasmic reticulum (SR).**

**A**, Effect of TAT-AKAP18 $\delta$ -C on pThr17-PLN in basal and during ISO-stimulation (5 min) in adult cardiomyocytes. pThr17-PLN, pSer16-PLN and PLN levels were detected by immunoblotting. Normal distribution was confirmed by Shapiro-Wilk test. Significant differences were examined by nested 1-way ANOVA with Tukey's multiple comparisons test ( $n=6-13$ , 4 rats). Effect of TAT-AKAP18 $\delta$ -C or a scramble control on decay time of Ca<sup>2+</sup> transients across a range of stimulation frequencies in adult cardiomyocytes in **(B)** absence or **(C)** presence of ISO. Normal distribution was confirmed by Shapiro-Wilk test (not tested for the 6 Hz data set with  $n<6$ ). Significant difference was examined by nested  $t$ -test,  $n=5-14$  in **B** (3-4 rats) and  $n=8-12$  in **C** (5-6 rats). Representative tracings are shown in Figure S6C and S6D. **D**, Effect of TAT-AKAP18 $\delta$ -C or a scrambled control on Ca<sup>2+</sup> reuptake rate in isolated mouse SR vesicles (left ventricle crude homogenate). Significant differences were examined by Wilcoxon matched-pairs signed rank test.

Immunoprecipitations employing CaMKII $\delta$ -T287A in the presence of CaM showed that AKAP18 $\delta$ -C also induced trapping of CaM to CaMKII $\delta$ -T287A (Figure 5F); a feature which has been similarly described for N2B-s.<sup>17</sup>

Kinetics of the AKAP18 $\delta$ -C (238-266)-CaMKII $\delta$  interaction analyzed by SPR revealed a dissociation equilibrium constant ( $K_D$ )=340 $\pm$ 46 nM, association rate constant ( $k_a$ )=(4.5 $\pm$ 1.0) $\times$ 10<sup>3</sup> M<sup>-1</sup> s<sup>-1</sup> and dissociation rate constant ( $k_d$ )=(1.4 $\pm$ 0.1) $\times$ 10<sup>-3</sup> s<sup>-1</sup> (Figure 5G). This indicated that the CaMKII $\delta$ -T287D-AKAP18 $\delta$ -C interaction is weaker than the CaMKII $\delta$ -T287D-AKAP18 $\delta$ -N interaction, has a slower on rate, and a faster off rate.

Taken together, our data indicate that AKAP18 $\delta$ -C is a CaMKII $\delta$  activator that lowers the Ca<sup>2+</sup> threshold for CaMKII $\delta$  activation (perhaps by keeping the inhibitory gate open) and also allows CaM trapping by the kinase (Figure 5H and 5I).

### AKAP18 $\delta$ -C Increases pThr17-PLN and Facilitates Faster SR Ca<sup>2+</sup> Reuptake

When introduced into adult rat cardiomyocytes, TAT-AKAP18 $\delta$ -C increased pThr17-PLN compared with both basal and isoproterenol-stimulated cardiomyocytes, and when combined with isoproterenol (5 minutes), the pThr17-PLN was further increased (tendency) (Figure 6A). pThr17-PLN was also augmented in neonatal rat cardiomyocytes treated with AKAP18 $\delta$ -C or N2B-s<sup>17</sup> (Figure S6A and S6B). No cytotoxicity was observed for AKAP18 $\delta$ -C or control peptide (Figure S3D).

Isolated adult rat cardiomyocytes were treated with cell-permeant TAT-AKAP18 $\delta$ -C or scrambled control peptides, in the presence and absence of isoproterenol. Ca<sup>2+</sup> transient recordings revealed findings opposite to those observed for AKAP18 $\delta$ -N, as TAT-AKAP18 $\delta$ -C accelerated Ca<sup>2+</sup> decline, both in the absence and

presence of isoproterenol (Figure 6B and 6C, representative tracings are shown in Figure S6C and S6D). This effect was most marked at low frequencies (1 and 4 Hz), as rising resting Ca<sup>2+</sup> levels, CaMKII $\delta$  activation, and increasing pThr17-PLN at higher pacing rates likely overpowered the effects of AKAP18 $\delta$ -C observed at baseline. Consistent with the data above, TAT-AKAP18 $\delta$ -C also increased the SERCA2 Ca<sup>2+</sup> uptake rate in isolated mouse SR vesicles (Figure 6D).

In summary, these data support the notion that by activating CaMKII $\delta$ , AKAP18 $\delta$ -C increases pThr17-PLN, and thereby accelerates Ca<sup>2+</sup> reuptake into the SR.

### AKAP18 $\delta$ Also Anchors and Functionally Regulates CaMKII $\delta$ Activity at RYR

RYR has been identified together with PLN-SERCA2 in SR nanodomains.<sup>28</sup> We therefore analyzed whether AKAP18 $\delta$  also regulates CaMKII $\delta$  activity at RYR. Colocalization and immunoprecipitation of CaMKII $\delta$  and RYR with AKAP18 $\delta$  in adult rat cardiomyocytes was shown using proximity ligation assay (Figure 7A and 7B, yellow spots) and Western blotting (Figure 7C). In similarity to effects on pThr17-PLN (Figure 3A), AKAP18 $\delta$ -N (55-98) also reduced CaMKII $\delta$  phosphorylation of Ser2814-RYR using biotin-ahx-RYR (2797-2827) as substrate (Figure 7D). When introduced into adult cardiomyocytes, cell-permeant TAT-AKAP18 $\delta$ -N (79-98) and TAT-AKAP18 $\delta$ -N (55-74) reduced Ser2814-RYR phosphorylation (Figure 7E) and RYR functional activity after isoproterenol stimulation (Figure 7G), whereas TAT-AKAP18 $\delta$ -C in the absence of isoproterenol exhibited opposite effects (Figure 7F and 7G). TAT-AKAP18 $\delta$ -N (79-98) exhibited no effect on pSer2814-RYR at basal level (Figure S7B) or at pSer2808-RYR after isoproterenol stimulation (Figure S7C), consistent with Ser2814 being the main CaMKII phosphorylation site in RYR.<sup>29</sup> Finally, we tested the effect of the AKAP18 $\delta$ -PLN competitor peptide on Ser2814-RYR phosphorylation. Contrary to pThr17-PLN (Figure 1C), no significant changes in the pSer2814-RYR level in cardiomyocytes treated with the AKAP18 $\delta$ -PLN competitor peptide were observed (Figure 7H). This finding indicates that RYR and PLN-SERCA2 might not compete for the same AKAP18 $\delta$ -CaMKII $\delta$  pool.

Taken together, our data indicate that in addition to effects at PLN-SERCA2, AKAP18 $\delta$  also anchors and regulates CaMKII $\delta$  activity at RYR.

## DISCUSSION

Here, we have provided mechanistic insight into the anchoring and regulation of CaMKII $\delta$  activity by AKAP18 $\delta$  at PLN-SERCA2 and RYR. We identified 2 unique regions in AKAP18 $\delta$  that inversely regulate CaMKII $\delta$  activity, CaMKII $\delta$ -catalyzed phosphorylation

of Thr17-PLN and Ser2814-RYR, and SERCA2 and RYR functional activities. We specifically showed that an inhibitory domain (AKAP18 $\delta$ -N) also binds calcified CaM, while an activating domain (AKAP18 $\delta$ -C) wedges CaMKII $\delta$  open, trapping CaM within the kinase, and lowering the Ca<sup>2+</sup> threshold for its activation.

### Working Model to Explain AKAP18 $\delta$ Effects on CaMKII $\delta$ in Myocytes

CaMKII activity has been shown to be sensitive to the frequency of Ca<sup>2+</sup> oscillations *in vitro*<sup>10</sup> and in intact adult cardiomyocytes.<sup>27</sup> Based on our data, we propose a working hypothesis whereby AKAP18 $\delta$  fine-tunes this frequency-dependent activation of CaMKII $\delta$ . At low stimulation frequency (Figure 8A), AKAP18 $\delta$ -N (in red) binds the CaMKII $\delta$  autoregulatory domain (pink), the ATP binding pocket, T- and S-site in the catalytic domain (green). This multipoint contact may stabilize the closed, inactive CaMKII conformation. Inhibition of the kinase persists. However, when the frequency of the Ca<sup>2+</sup> transients increases (Figure 8B), accumulated calcified CaM (beige) may outcompete the inhibitory AKAP18 $\delta$ -N-CaMKII $\delta$  interaction by binding to the CaMKII $\delta$  autoregulatory domain (pink) and AKAP18 $\delta$ -N (red). These events lead to displacement of the S-site from AKAP18 $\delta$ -N. CaM binding to AKAP18 $\delta$ -N may alter its conformation, leading to its release also from the ATP-binding region and T-site (Figure 8B), augmented access of Thr17-PLN to the S-site, and greater CaMKII $\delta$  potency. Concomitantly, AKAP18 $\delta$ -C (in green) binds to the released T-site, keeping the inhibitory gate open as a wedge. This potentiates CaMKII $\delta$  by lowering the Ca<sup>2+</sup> threshold for its activation and by trapping CaM, leading to substrate phosphorylation (eg, Thr287 in the neighboring CaMKII $\delta$  subunit, Thr17-PLN or Ser2814-RYR) during subsequent Ca<sup>2+</sup> transients in a feed-forward manner: molecular memory of CaMKII $\delta$  results. Thereafter, when the frequency of Ca<sup>2+</sup> transients declines, CaM dissociates from CaMKII $\delta$  and AKAP18 $\delta$ -N, making the latter accessible to bind the CaMKII $\delta$  autoregulatory domain, ATP binding region, and S- and T-sites, leading to re-inhibition of CaMKII $\delta$  (Figure 8A). While plausible, it is unknown whether in the intact continuously beating heart the activating effect of AKAP18 $\delta$ -C is dominant over the inhibitory stabilization caused by AKAP18 $\delta$ -N.

In contrast to the CaMKII $\delta$  autoregulatory domain, AKAP18 $\delta$ -N does not contain the cluster of Phe293, Asn294, and Arg296, which is critical for CaM trapping by CaMKII $\delta$ ,<sup>22</sup> suggesting that AKAP18 $\delta$ -N does not trap calcified CaM as the Ca<sup>2+</sup> transient frequency declines. This may allow AKAP18 $\delta$ -N to inhibit CaMKII $\delta$  before complete dissociation of CaM from CaMKII $\delta$ . In fact, since AKAP18 $\delta$ -C and AKAP18 $\delta$ -N (55-74) bind differently within the T-site region, there might not be any need for AKAP18 $\delta$ -C to dissociate from CaMKII $\delta$

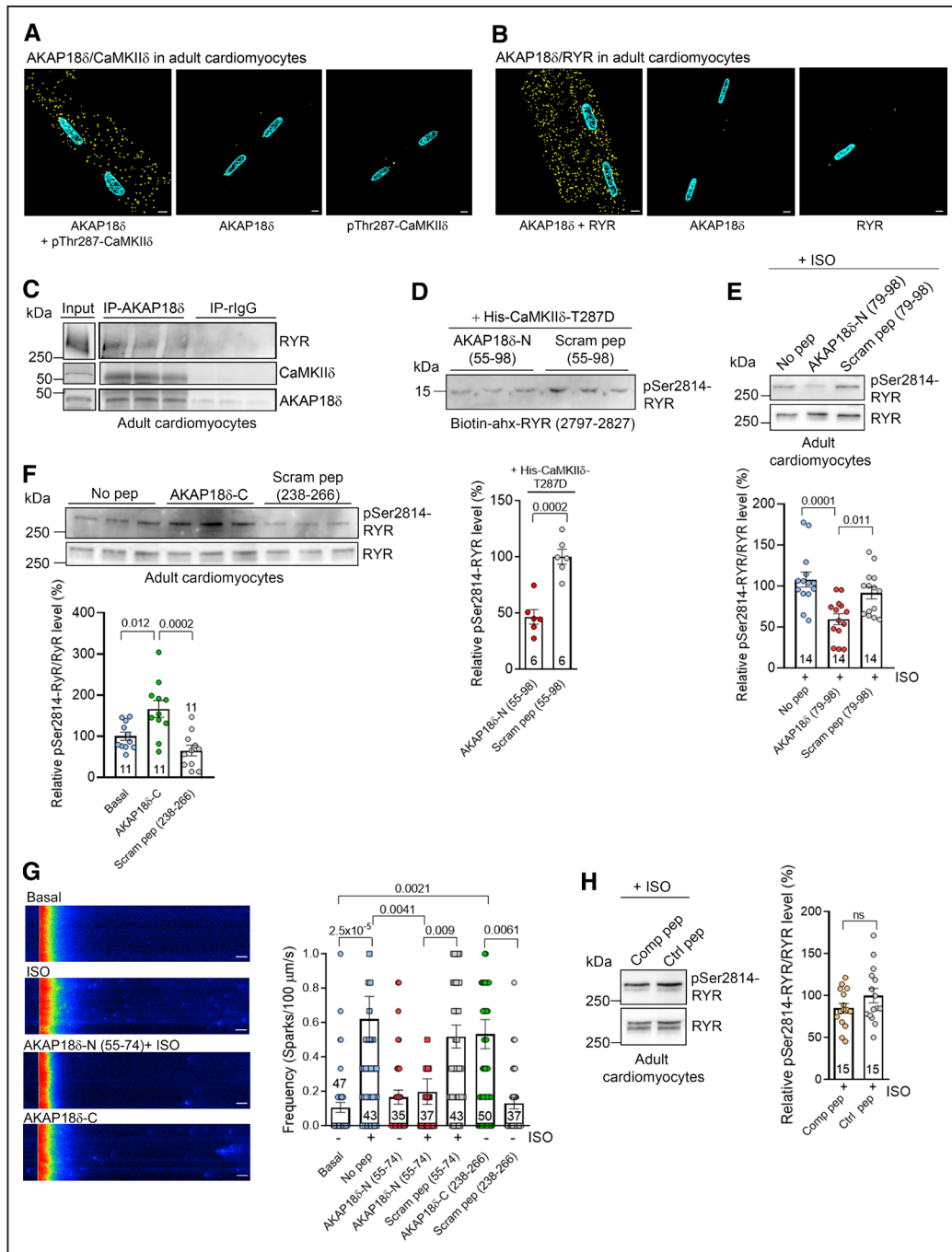


**Figure 7. AKAP18 $\delta$  (A-kinase anchoring protein 18 $\delta$ ) anchors and functionally regulates CaMKII $\delta$  activity also at ryanodine receptor (RyR).**

**A**, In situ proximity ligation assay of **(A)** AKAP18 $\delta$ -pThr287-CaMKII $\delta$  and **(B)** AKAP18 $\delta$ -RyR (yellow dots in left panels) in adult cardiomyocytes (see Materials and Methods section for detailed description). Incubations with only anti-AKAP18 $\delta$ , anti-pThr287-CaMKII $\delta$ , or anti-RyR were used as negative controls (middle and right panels). Positive control for the assay is shown in [Figure S7A](#). Scale bars=5  $\mu$ m. **C**, Immunoprecipitation of AKAP18 $\delta$ -CaMKII $\delta$ -RyR in adult cardiomyocyte lysate detected by immunoblotting. **D**, CaMKII $\delta$  phosphorylation of biotin-ahx-RyR (2797-2827), with or without presence of AKAP18 $\delta$ -N (55-98) or the scrambled control. Biotin-ahx-pSer2814-RyR was detected by immunoblotting. Normal distribution was confirmed by Shapiro-Wilk test, and significant differences were examined by unpaired *t* test  $n=6$ . pSer2814-RyR and RyR levels in adult cardiomyocytes treated with **(E)** TAT-AKAP18 $\delta$ -N (79-98) in presence of ISO or **(F)** AKAP18 $\delta$ -C (238-266) in absence of ISO. The respective scrambled peptides were used as controls. Normal distribution was confirmed by Shapiro-Wilk test (in **E** and **F**). Significant differences examined by the linear mixed effect model from the R nlme package with Tukey post hoc correction ( $n=14$ , 5 rats in **E**, and  $n=11$ , 4 rats in **F**). **G**, Line scans and Ca<sup>2+</sup> sparks of cardiomyocytes treated with or without ISO, TAT-AKAP18 $\delta$ -N (55-74), AKAP18 $\delta$ -C (238-266) or the respective scrambled control peptides. Significant differences examined by the linear mixed effect model from the R nlme package with Tukey post hoc correction ( $n=35-50$ , 5 rats). Scale bars=150 ms. **H**, Immunoblotting of pSer2814-RyR and RyR in ISO-stimulated cardiomyocytes pretreated with the cell-permeant AKAP18 $\delta$ -PLN competitor or control peptide. Normal distribution was confirmed by Shapiro-Wilk test. Ns, not significant, examined by nested *t* test ( $n=12$ , 5 rats).

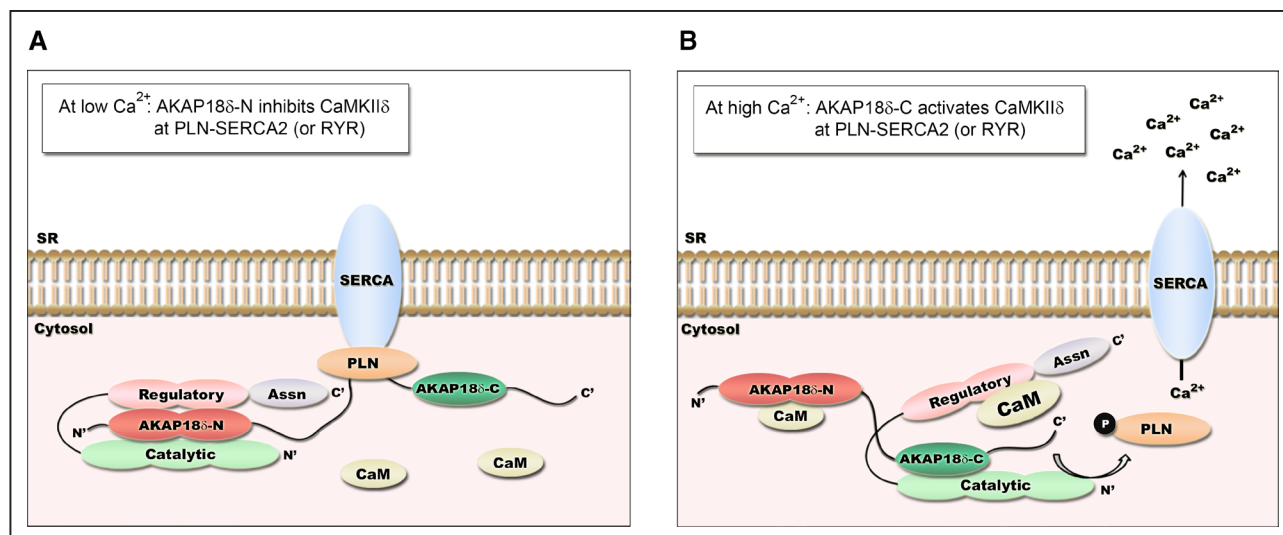


**Figure 8. A model where the 2 unique regions in AKAP18 $\delta$  (A-kinase anchoring protein 18 $\delta$ ) fine-tune CaMKII $\delta$  activation at PLN (phospholamban)-sarcoplasmic reticulum (SR) Ca<sup>2+</sup>-ATPase 2 (SERCA2 or ryanodine receptor [RYR]).**

**A**, At low  $\text{Ca}^{2+}$  transient frequency, AKAP18 $\delta$ -N (red) inhibits CaMKII $\delta$  by binding to the regulatory domain (pink), and ATP-binding pocket, T- and S-sites in the catalytic domain (green). No Thr17-PLN (or Ser2814-RYR) phosphorylation results. **B**, When the  $\text{Ca}^{2+}$  transient frequency increases, accumulated calcified CaM (beige) outcompetes the inhibitory AKAP18 $\delta$ -CaMKII $\delta$  interaction by binding to the regulatory domain (pink) and AKAP18 $\delta$ -N (red). AKAP18 $\delta$ -C (dark green) binds to the released T-site in CaMKII $\delta$  and lowers the  $\text{Ca}^{2+}$  threshold for kinase activation, by keeping the inhibitory gate open and trapping CaM within CaMKII $\delta$ . CaMKII $\delta$  catalyzes further Thr17-PLN (or Ser2814-RYR) phosphorylation, leading to reduced PLN association and faster SR  $\text{Ca}^{2+}$  reuptake by SERCA2 (or  $\text{Ca}^{2+}$  release by RYR). It is also possible that AKAP18 $\delta$ -N and AKAP18 $\delta$ -C regulate 2 different CaMKII molecules. Assn indicates association domain.

when the frequency declines. With this positioning, AKAP18 $\delta$ -C might rapidly potentiate kinase activity during a subsequent rise in  $\text{Ca}^{2+}$  transient frequency since this could occur as soon as AKAP18 $\delta$ -N dissociates, and independently of the Thr287 autophosphorylation state or other posttranslational modifications reported to promote autonomous activation of CaMKII.<sup>30–33</sup> In the presence of posttranslational modifications, AKAP18 $\delta$ -C may increase CaMKII $\delta$  activation to an even higher level, whereas AKAP18 $\delta$ -N is expected to still be able to inhibit CaMKII $\delta$  (illustrated in Figure 2I), even if its binding to the autoregulatory domain is abolished by oxidation (Met281/282)<sup>30</sup> or S-nitrosylation (Cys290).<sup>33</sup> The stoichiometry of the AKAP18 $\delta$ -CaMKII $\delta$  interaction is not known, but since AKAP18 $\delta$  has been shown to oligomerize,<sup>34</sup> it is plausible that several AKAP18 $\delta$  molecules anchor and regulate different CaMKII $\delta$  monomers within the same CaMKII oligomer. Bioinformatics revealed that the AKAP18 $\delta$ -binding regions are well conserved across CaMKII isoforms (Figure S8), suggesting that AKAP18 $\delta$  may be able to anchor and regulate different CaMKII isoforms, and might provide an explanation for some Thr17-PLN phosphorylation observed in the CaMKII $\delta$  knock out mouse model.<sup>35</sup>

Additional studies are needed to further interrogate the proposed AKAP18 $\delta$ -CaMKII $\delta$ -SERCA2-PLN/RYR model (Figure 8). Both PLN and RYR are thought to be important targets for CaMKII $\delta$  effects during the force frequency relationship.<sup>29,36–38</sup> While the effects of CaMKII and PLN on frequency-dependent acceleration

of relaxation have been more controversial,<sup>39,44,45</sup> recent works employing transgenic CaMKII inhibition in PLN-deficient mice have indicated that CaMKII-dependent regulation of PLN is critical to achieve frequency-dependent acceleration of relaxation, but that as yet unidentified CaMKII targets may also contribute.<sup>38</sup> Our data support an important role of CaMKII during frequency-dependent acceleration of relaxation, as we also observed that AKAP18 $\delta$ -C-dependent CaMKII stimulation accelerated  $\text{Ca}^{2+}$  transient decline at low stimulation frequency (Figure 6B).

### AKAP18 $\delta$ Is a Novel CaMKII Anchoring Protein

To our knowledge, this is the first AKAP (A-kinase anchoring protein) reported to anchor a CaMKII isoform, defining AKAP18 $\delta$  also as a CaM-KAP. From the crystal structures of fragments of AKAP18 $\delta$ <sup>46</sup> and AKAP18 $\gamma$ ,<sup>42</sup> it appears as though the 2 CaMKII $\delta$ -binding sites are mostly accessible and do not overlap with the PLN<sup>14</sup> or PKA<sup>13</sup> binding sites. Thus, both CaMKII $\delta$  and PKA may bind to AKAP18 $\delta$  and phosphorylate PLN at the same time. AKAP18 $\delta$  also coordinates phosphorylation of inhibitor-1,<sup>47</sup> which in turn inhibits protein phosphatase 1, the major phosphatase responsible for dephosphorylating PLN.<sup>43,48,49</sup>

It remains to be determined whether the opposing effects of the 2 AKAP18 $\delta$  regions on CaMKII $\delta$  activity are unique to AKAP18 $\delta$ , or whether a similar arrangement exists in other proteins. CaMKII $\alpha$  interacts with

2 sites in the N-methyl-D-aspartate receptor subunit NR2B.<sup>17</sup> One site (N2B-s) is similar to AKAP18δ-C, both at sequence level, as well as functionally, as it generates autonomous activation of CaMKIIα.<sup>17</sup> The second-binding site is reported to be CaMKIIα-Thr286 dependent.<sup>17</sup> Densin, located in neuronal postsynaptic densities, also inhibits CaMKII-mediated phosphorylation through T-site binding<sup>18</sup> but binds to the CaMKII association domain through a second site.<sup>50–52</sup> Furthermore, GTPase Rem2, a critical regulator of dendritic branching and homeostatic plasticity, binds also to the association domain, but inhibits CaMKII rather through the S-site.<sup>20</sup> Interestingly, Rem2 also interacts with CaM.<sup>53,54</sup>

## Pathophysiological Relevance

Understanding the molecular mechanisms of CaMKII regulation is important in the context of various heart diseases and the development of new treatment strategies. Sustained CaMKII activation is linked to impaired cardiomyocyte Ca<sup>2+</sup> homeostasis, cardiac dysfunction, and arrhythmias in diseases spanning atrial fibrillation, heart failure, and diabetic cardiomyopathy. Although CaMKII activity and RYR functional activity are often increased in these conditions,<sup>4</sup> decreased SERCA2 activity is often reported. During heart failure, reduction in SERCA2 activity is likely a result of both lowered protein expression<sup>55</sup> and hypophosphorylation of PLN following increased phosphatase activity.<sup>56,57</sup> Restoration of SR Ca<sup>2+</sup> re-uptake through increasing PLN phosphorylation levels and/or SERCA2 activity is therefore considered to be a potential therapeutic strategy.<sup>58,59</sup> Future studies are needed to test whether the CaMKII activator peptide identified in this study (AKAP18δ-C) can be used to increase pThr17-PLN levels and thus SERCA2 activity in vivo. One strategy may be to target AKAP18δ-C to longitudinal SR, using a strategy similar to that described for the AIP<sub>4</sub>-longitudinal SR transgenic mice.<sup>5,60</sup> To this end, the peptide sequences presently derived from the 2 AKAP18δ regions should be viewed as novel reagents that may help identify new CaMKII targets and approaches to therapeutically modify CaMKII activity and cardiomyocyte Ca<sup>2+</sup> cycling.

## ARTICLE INFORMATION

Received August 10, 2020; revision received November 18, 2021; accepted November 22, 2021.

### Affiliations

Institute for Experimental Medical Research, Oslo University Hospital and University of Oslo, Norway (C.R.C., J.M.A., A.B.-D., M.L., P.K.L., H.J., P.W., T.R.S.K., G.C., I.S., X.S., W.E.L., O.M.S.). The KG Jebsen Cardiac Research Center, University of Oslo, Norway (A.B.-D., M.L., P.K.L., T.R.S.K., G.C., I.S., X.S., W.E.L., O.M.S.). Department of Molecular Medicine, Institute of Basic Medical Sciences, University of Oslo Norway (J.M.A.). Department of Pharmacology, Oslo University Hospital, Norway (J.M.A.). Max-Delbrück-Center for Molecular Medicine in the Helmholtz Association (MDC), Berlin, Germany (M.C.M., E.K.). Department of Pharmacology, University of California at Davis (L.P., D.M.B.). Department of Microbiology, Oslo University

Hospital, Norway (B.D.). Department of Medical Biochemistry, Institute for Clinical Medicine, University of Oslo, Norway (B.D.). Institute of Experimental Cardiovascular Research, University Medical Center Hamburg-Eppendorf, Hamburg, Germany (H.S., V.N.). German Centre for Cardiovascular Research, Partner Site Hamburg/Kiel/Lübeck, Germany (H.S., S.H., O.J.M., V.N.). Department of Internal Medicine III, University of Kiel, Kiel, Germany (S.H., O.J.M.). German Centre for Cardiovascular Research (DZHK), Partner Site Berlin, Germany (E.K.).

### Acknowledgment

We thank Dr Ryan Walker-Gray for critically reading the article.

### Sources of Funding

This work was supported by the Norwegian Research Council, UNIFORMED, Norwegian Health Association, Anders Jahre's Fund for the Promotion of Science, Stiftelsen Kristian Gerhard Jebsen, Norway, HSØ Regional Core Facility for Structural Biology (2015095), and the National Institutes of Health (R01-HL133832 and R01-HL142282) to D.M. Bers. E. Klussmann was supported by the Deutsche Forschungsgemeinschaft (DFG; KL1415/7-1, and the program-project grant, 394046635 – SFB 1365), the Bundesministerium für Bildung und Forschung (BMBF; 16GW0179K), and the German Israeli Foundation (GIF, I-1452-203/13-2018).

### Disclosures

C.R. Carlson, J.M. Aronsen, W.E. Louch, E. Klussmann, and O.M. Sejersted are partners in 2 Disclosure of inventions regarding the CaMKII activator and inhibitor peptides.

### Supplemental Material

Expanded Materials and Methods  
Figures S1–S8  
References 61–75

## REFERENCES

- Bers DM. Cardiac excitation-contraction coupling. *Nature*. 2002;415:198–205. doi: 10.1038/415198a
- Bers DM. Altered cardiac myocyte Ca regulation in heart failure. *Physiology (Bethesda)*. 2006;21:380–387. doi: 10.1152/physiol.00019.2006
- Maier LS, Bers DM. Role of Ca<sup>2+</sup>/calmodulin-dependent protein kinase (CaMK) in excitation-contraction coupling in the heart. *Cardiovasc Res*. 2007;73:631–640. doi: 10.1016/j.cardiores.2006.11.005
- Mattiazzi A, Kranias EG. The role of CaMKII regulation of phospholamban activity in heart disease. *Front Pharmacol*. 2014;5:5. doi: 10.3389/fphar.2014.00005
- Ji Y, Zhao W, Li B, Desantiago J, Picht E, Kaetzel MA, Schultz Jel J, Kranias EG, Bers DM, Dedman JR. Targeted inhibition of sarcoplasmic reticulum CaMKII activity results in alterations of Ca<sup>2+</sup> homeostasis and cardiac contractility. *Am J Physiol Heart Circ Physiol*. 2006;290:H599–H606. doi: 10.1152/ajpheart.00214.2005
- Rosenberg OS, Deindl S, Sung RJ, Nairn AC, Kuriyan J. Structure of the autoinhibited kinase domain of CaMKII and SAXS analysis of the holoenzyme. *Cell*. 2005;123:849–860. doi: 10.1016/j.cell.2005.10.029
- Hudmon A, Schulman H. Structure-function of the multifunctional Ca<sup>2+</sup>/calmodulin-dependent protein kinase II. *Biochem J*. 2002;364(pt 3):593–611. doi: 10.1042/BJ20020228
- Meyer T, Hanson PI, Stryer L, Schulman H. Calmodulin trapping by calcium-calmodulin-dependent protein kinase. *Science*. 1992;256:1199–1202. doi: 10.1126/science.256.5060.1199
- Miller SG, Patton BL, Kennedy MB. Sequences of autophosphorylation sites in neuronal type II CaM kinase that control Ca<sup>2+</sup>-independent activity. *Neuron*. 1988;1:593–604. doi: 10.1016/0896-6273(88)90109-2
- De Koninck P, Schulman H. Sensitivity of CaM kinase II to the frequency of Ca<sup>2+</sup> oscillations. *Science*. 1998;279:227–230. doi: 10.1126/science.279.5348.227
- Saucerman JJ, Bers DM. Calmodulin mediates differential sensitivity of CaMKII and calcineurin to local Ca<sup>2+</sup> in cardiac myocytes. *Biophys J*. 2008;95:4597–4612. doi: 10.1529/biophysj.108.128728
- Wood BM, Simon M, Galice S, Alim CC, Ferrero M, Pinna NN, Bers DM, Bossuyt J. Cardiac CaMKII activation promotes rapid translocation to its extra-dyadic targets. *J Mol Cell Cardiol*. 2018;125:18–28. doi: 10.1016/j.yjmcc.2018.10.010
- Henn V, Edemir B, Stefan E, Wiesner B, Lorenz D, Theilig F, Schmitt R, Vossebein L, Tamma G, Beyermann M, et al. Identification of a novel



- A-kinase anchoring protein 18 isoform and evidence for its role in the vasopressin-induced aquaporin-2 shuttle in renal principal cells. *J Biol Chem*. 2004;279:26654–26665. doi: 10.1074/jbc.M312835200
14. Lygren B, Carlson CR, Santamaria K, Lissandron V, McSorley T, Litzenberg J, Lorenz D, Wiesner B, Rosenthal W, Zaccolo M, et al. AKAP complex regulates Ca<sup>2+</sup> re-uptake into heart sarcoplasmic reticulum. *EMBO Rep*. 2007;8:1061–1067. doi: 10.1038/sj.embor.7401081
  15. Ahmad F, Shen W, Vandeput F, Szabo-Fresnais N, Krall J, Degerman E, Goetz F, Klusmann E, Movsesian M, Manganiello V. Regulation of sarcoplasmic reticulum Ca<sup>2+</sup> ATPase 2 (SERCA2) activity by phosphodiesterase 3A (PDE3A) in human myocardium: phosphorylation-dependent interaction of PDE3A1 with SERCA2. *J Biol Chem*. 2015;290:6763–6776. doi: 10.1074/jbc.M115.638585
  16. Fong YL, Taylor WL, Means AR, Soderling TR. Studies of the regulatory mechanism of Ca<sup>2+</sup>/calmodulin-dependent protein kinase II. Mutation of threonine 286 to alanine and aspartate. *J Biol Chem*. 1989;264:16759–16763.
  17. Bayer KU, De Koninck P, Leonard AS, Hell JW, Schulman H. Interaction with the NMDA receptor locks CaMKII in an active conformation. *Nature*. 2001;411:801–805. doi: 10.1038/35081080
  18. Jiao Y, Jalan-Sakrikar N, Robison AJ, Baucum AJ 2<sup>nd</sup>, Bass MA, Colbran RJ. Characterization of a central Ca<sup>2+</sup>/calmodulin-dependent protein kinase II alpha/beta binding domain in densin that selectively modulates glutamate receptor subunit phosphorylation. *J Biol Chem*. 2011;286:24806–24818. doi: 10.1074/jbc.M110.216010
  19. Yang E, Schulman H. Structural examination of autoregulation of multifunctional calcium/calmodulin-dependent protein kinase II. *J Biol Chem*. 1999;274:26199–26208. doi: 10.1074/jbc.274.37.26199
  20. Royer L, Herzog JJ, Kenny K, Tzvetkova B, Cochrane JC, Marr MT II, Paradis S. The Ras-like GTPase Rem2 is a potent inhibitor of calcium/calmodulin-dependent kinase II activity. *J Biol Chem*. 2018;293:14798–14811. doi: 10.1074/jbc.RA118.003560
  21. Vest RS, Davies KD, O'Leary H, Port JD, Bayer KU. Dual mechanism of a natural CaMKII inhibitor. *Mol Biol Cell*. 2007;18:5024–5033. doi: 10.1091/mbc.e07-02-0185
  22. Singla SI, Hudmon A, Goldberg JM, Smith JL, Schulman H. Molecular characterization of calmodulin trapping by calcium/calmodulin-dependent protein kinase II. *J Biol Chem*. 2001;276:29353–29360. doi: 10.1074/jbc.M101744200
  23. James P, Vorherr T, Carafoli E. Calmodulin-binding domains: just two faced or multi-faceted? *Trends Biochem Sci*. 1995;20:38–42. doi: 10.1016/s0968-0004(00)88949-5
  24. Faux MC, Scott JD. Regulation of the AKAP79-protein kinase C interaction by Ca<sup>2+</sup>/Calmodulin. *J Biol Chem*. 1997;272:17038–17044. doi: 10.1074/jbc.272.27.17038
  25. Strack S, Colbran RJ. Autophosphorylation-dependent targeting of calcium/calmodulin-dependent protein kinase II by the NR2B subunit of the N-methyl-D-aspartate receptor. *J Biol Chem*. 1998;273:20689–20692. doi: 10.1074/jbc.273.33.20689
  26. Strack S, McNeill RB, Colbran RJ. Mechanism and regulation of calcium/calmodulin-dependent protein kinase II targeting to the NR2B subunit of the N-methyl-D-aspartate receptor. *J Biol Chem*. 2000;275:23798–23806. doi: 10.1074/jbc.M001471200
  27. Erickson JR, Patel R, Ferguson A, Bossuyt J, Bers DM. Fluorescence resonance energy transfer-based sensor Camui provides new insight into mechanisms of calcium/calmodulin-dependent protein kinase II activation in intact cardiomyocytes. *Circ Res*. 2011;109:729–738. doi: 10.1161/CIRCRESAHA.111.247148
  28. Alsina KM, Hulsurkar M, Brandenburg S, Kownatzki-Danger D, Lenz C, Urlaub H, Abu-Taha I, Kamler M, Chiang DY, Lahiri SK, et al. Loss of protein phosphatase 1 regulatory subunit PPP1R3A promotes atrial fibrillation. *Circulation*. 2019;140:681–693. doi: 10.1161/CIRCULATIONAHA.119.039642
  29. Wehrens XH, Lehnart SE, Reiken SR, Marks AR. Ca<sup>2+</sup>/calmodulin-dependent protein kinase II phosphorylation regulates the cardiac ryanodine receptor. *Circ Res*. 2004;94:e61–e70. doi: 10.1161/01.RES.0000125626.33738.E2
  30. Erickson JR, Joiner ML, Guan X, Kutschke W, Yang J, Oddis CV, Bartlett RK, Lowe JS, O'Donnell SE, Aykin-Burns N, et al. A dynamic pathway for calcium-independent activation of CaMKII by methionine oxidation. *Cell*. 2008;133:462–474. doi: 10.1016/j.cell.2008.02.048
  31. Erickson JR, Pereira L, Wang L, Han G, Ferguson A, Dao K, Copeland RJ, Despa F, Hart GW, Ripplinger CM, et al. Diabetic hyperglycaemia activates CaMKII and arrhythmias by O-linked glycosylation. *Nature*. 2013;502:372–376. doi: 10.1038/nature12537
  32. Coultrap SJ, Bayer KU. Nitric oxide induces Ca<sup>2+</sup>-independent activity of the Ca<sup>2+</sup>/calmodulin-dependent protein kinase II (CaMKII). *J Biol Chem*. 2014;289:19458–19465. doi: 10.1074/jbc.M114.558254
  33. Erickson JR, Nichols CB, Uchinoumi H, Stein ML, Bossuyt J, Bers DM. S-Nitrosylation induces both autonomous activation and inhibition of calcium/calmodulin-dependent protein kinase II  $\delta$ . *J Biol Chem*. 2015;290:25646–25656. doi: 10.1074/jbc.M115.650234
  34. Singh A, Rigatti M, Le AV, Carlson CR, Moraru II, Dodge-Kafka KL. Analysis of AKAP7 $\gamma$  dimerization. *J Signal Transduct*. 2015;2015:371626. doi: 10.1155/2015/371626
  35. Grimm M, Ling H, Brown JH. Crossing signals: relationships between  $\beta$ -adrenergic stimulation and CaMKII activation. *Heart Rhythm*. 2011;8:1296–1298. doi: 10.1016/j.hrthm.2011.02.027
  36. Bluhm WF, Kranias EG, Dillmann WH, Meyer M. Phospholamban: a major determinant of the cardiac force-frequency relationship. *Am J Physiol Heart Circ Physiol*. 2000;278:H249–H255. doi: 10.1152/ajpheart.2000.278.1.H249
  37. Kushnir A, Shan J, Betzenhauser MJ, Reiken S, Marks AR. Role of CaMKII $\delta$  phosphorylation of the cardiac ryanodine receptor in the force frequency relationship and heart failure. *Proc Natl Acad Sci U S A*. 2010;107:10274–10279. doi: 10.1073/pnas.1005843107
  38. Wu Y, Luczak ED, Lee EJ, Hidalgo C, Yang J, Gao Z, Li J, Wehrens XH, Granzier H, Anderson ME. CaMKII effects on inotropic but not lusitropic force frequency responses require phospholamban. *J Mol Cell Cardiol*. 2012;53:429–436. doi: 10.1016/j.yjmcc.2012.06.019
  39. DeSantiago J, Maier LS, Bers DM. Frequency-dependent acceleration of relaxation in the heart depends on CaMKII, but not phospholamban. *J Mol Cell Cardiol*. 2002;34:975–984. doi: 10.1006/jmcc.2002.2034
  40. Zhao W, Uehara Y, Chu G, Song Q, Qian J, Young K, Kranias EG. Threonine-17 phosphorylation of phospholamban: a key determinant of frequency-dependent increase of cardiac contractility. *J Mol Cell Cardiol*. 2004;37:607–612. doi: 10.1016/j.yjmcc.2004.05.013
  41. Louch WE, Stokke MK, Sjaastad I, Christensen G, Sejersted OM. No rest for the weary: diastolic calcium homeostasis in the normal and failing myocardium. *Physiology (Bethesda)*. 2012;27:308–323. doi: 10.1152/physiol.00021.2012
  42. Bjerregaard-Andersen K, Ostensen E, Scott JD, Tasken K, Morth JP. Malonate in the nucleotide-binding site traps human AKAP18 gamma/delta in a novel conformational state. *Acta Crystallogr F*. 2016;72:591–597. doi: 10.1107/S2053230X16010189
  43. Pathak A, del Monte F, Zhao W, Schultz JE, Lorenz JN, Bodi I, Weiser D, Hahn H, Carr AN, Syed F, et al. Enhancement of cardiac function and suppression of heart failure progression by inhibition of protein phosphatase 1. *Circ Res*. 2005;96:756–766. doi: 10.1161/01.RES.0000161256.85833.f.a
  44. Valverde CA, Mundiña-Weilenmann C, Said M, Ferrero P, Vittone L, Salas M, Palomeque J, Petroff MV, Mattiazzi A. Frequency-dependent acceleration of relaxation in mammalian heart: a property not relying on phospholamban and SERCA2a phosphorylation. *J Physiol*. 2005;562(pt 3):801–813. doi: 10.1113/jphysiol.2004.075432
  45. Picht E, DeSantiago J, Huke S, Kaetzel MA, Dedman JR, Bers DM. CaMKII inhibition targeted to the sarcoplasmic reticulum inhibits frequency-dependent acceleration of relaxation and Ca<sup>2+</sup> current facilitation. *J Mol Cell Cardiol*. 2007;42:196–205. doi: 10.1016/j.yjmcc.2006.09.007
  46. Gold MG, Smith FD, Scott JD, Barford D. AKAP18 contains a phosphatase domain that binds AMP. *J Mol Biol*. 2008;375:1329–1343. doi: 10.1016/j.jmb.2007.11.037
  47. Singh A, Redden JM, Kapiloff MS, Dodge-Kafka KL. The large isoforms of A-kinase anchoring protein 18 mediate the phosphorylation of inhibitor-1 by protein kinase A and the inhibition of protein phosphatase 1 activity. *Mol Pharmacol*. 2011;79:533–540. doi: 10.1124/mol.110.065425
  48. Carr AN, Schmidt AG, Suzuki Y, del Monte F, Sato Y, Lanner C, Breiden K, Jing SL, Allen PB, Greengard P, et al. Type 1 phosphatase, a negative regulator of cardiac function. *Mol Cell Biol*. 2002;22:4124–4135. doi: 10.1128/MCB.22.12.4124-4135.2002
  49. Nicolaou P, Hajjar RJ, Kranias EG. Role of protein phosphatase-1 inhibitor-1 in cardiac physiology and pathophysiology. *J Mol Cell Cardiol*. 2009;47:365–371. doi: 10.1016/j.yjmcc.2009.05.010
  50. Strack S, Robison AJ, Bass MA, Colbran RJ. Association of calcium/calmodulin-dependent kinase II with developmentally regulated splice variants of the postsynaptic density protein densin-180. *J Biol Chem*. 2000;275:25061–25064. doi: 10.1074/jbc.C000319200
  51. McNeill RB, Colbran RJ. Interaction of autophosphorylated Ca<sup>2+</sup>/calmodulin-dependent protein kinase II with neuronal cytoskeletal proteins.

- Characterization of binding to a 190-kDa postsynaptic density protein. *J Biol Chem*. 1995;270:10043–10049. doi: 10.1074/jbc.270.17.10043
52. Walikonis RS, Oguni A, Khorosheva EM, Jeng CJ, Asuncion FJ, Kennedy MB. Densin-180 forms a ternary complex with the (alpha)-subunit of Ca<sup>2+</sup>/calmodulin-dependent protein kinase II and (alpha)-actinin. *J Neurosci*. 2001;21:423–433.
  53. Béguin P, Mahalakshmi RN, Nagashima K, Cher DH, Kuwamura N, Yamada Y, Seino Y, Hunziker W. Roles of 14-3-3 and calmodulin binding in subcellular localization and function of the small G-protein Rem2. *Biochem J*. 2005;390(pt 1):67–75. doi: 10.1042/BJ20050414
  54. Flynn R, Labrie-Dion E, Bernier N, Colicos MA, De Koninck P, Zamponi GW. Activity-dependent subcellular cotrafficking of the small GTPase Rem2 and Ca<sup>2+</sup>/CaM-dependent protein kinase II $\alpha$ . *PLoS One*. 2012;7:e41185. doi: 10.1371/journal.pone.0041185
  55. Stüdeli R, Jung S, Mohacs P, Perruchoud S, Castiglioni P, Wenaweser P, Heimbeck G, Feller M, Hullin R. Diastolic dysfunction in human cardiac allografts is related with reduced SERCA2a gene expression. *Am J Transplant*. 2006;6:775–782. doi: 10.1111/j.1600-6143.2006.01241.x
  56. Schwinger RH, Münch G, Bölk B, Karczewski P, Krause EG, Erdmann E. Reduced Ca(2+)-sensitivity of SERCA 2a in failing human myocardium due to reduced serin-16 phospholamban phosphorylation. *J Mol Cell Cardiol*. 1999;31:479–491. doi: 10.1006/jmcc.1998.0897
  57. Münch G, Bölk B, Karczewski P, Schwinger RH. Evidence for calcineurin-mediated regulation of SERCA 2a activity in human myocardium. *J Mol Cell Cardiol*. 2002;34:321–334. doi: 10.1006/jmcc.2001.1515
  58. del Monte F, Hajjar RJ. Targeting calcium cycling proteins in heart failure through gene transfer. *J Physiol*. 2003;546(pt 1):49–61. doi: 10.1113/jphysiol.2002.026732
  59. Lipskaia L, Chemaly ER, Hadri L, Lompre AM, Hajjar RJ. Sarcoplasmic reticulum Ca(2+) ATPase as a therapeutic target for heart failure. *Expert Opin Biol Ther*. 2010;10:29–41. doi: 10.1517/14712590903321462
  60. Ji Y, Li B, Reed TD, Lorenz JN, Kaetzel MA, Dedman JR. Targeted inhibition of Ca<sup>2+</sup>/calmodulin-dependent protein kinase II in cardiac longitudinal sarcoplasmic reticulum results in decreased phospholamban phosphorylation at threonine 17. *J Biol Chem*. 2003;278:25063–25071. doi: 10.1074/jbc.M302193200
  61. Mathiesen SB, Lunde M, Aronsen JM, Romaine A, Kaupang A, Martinsen M, de Souza GA, Nyman TA, Sjaastad I, Christensen G, et al. The cardiac syndecan-4 interactome reveals a role for syndecan-4 in nuclear translocation of muscle LIM protein (MLP). *J Biol Chem*. 2019;294:8717–8731. doi: 10.1074/jbc.RA118.006423
  62. Werfel S, Jungmann A, Lehmann L, Ksienzyk J, Bekerredjian R, Kaya Z, Leuchs B, Nordheim A, Backs J, Engelhardt S, et al. Rapid and highly efficient inducible cardiac gene knockout in adult mice using AAV-mediated expression of Cre recombinase. *Cardiovasc Res*. 2014;104:15–23. doi: 10.1093/cvr/cvu174
  63. Jungmann A, Leuchs B, Rommelaere J, Katus HA, Müller OJ. Protocol for efficient generation and characterization of adeno-associated viral vectors. *Hum Gene Ther Methods*. 2017;28:235–246. doi: 10.1089/hgtb.2017.192
  64. Börner S, Schwede F, Schlipp A, Berisha F, Calebiro D, Lohse MJ, Nikolaev VO. FRET measurements of intracellular cAMP concentrations and cAMP analog permeability in intact cells. *Nat Protoc*. 2011;6:427–438. doi: 10.1038/nprot.2010.198
  65. Li JL, Wang XN, Fraser SF, Wrigley TV, McKenna MJ. Effects of fatigue and training on sarcoplasmic reticulum Ca(2+) regulation in human skeletal muscle. *J Appl Physiol (1985)*. 2002;92:912–922. doi: 10.1152/jappphysiol.00643.2000
  66. O'Brien PJ. Calcium sequestration by isolated sarcoplasmic reticulum: real-time monitoring using ratiometric dual-emission spectrofluorometry and the fluorescent calcium-binding dye indo-1. *Mol Cell Biochem*. 1990;94:113–119. doi: 10.1007/BF00214118
  67. Kolstad TR, van den Brink J, MacQuaide N, Lunde PK, Frisk M, Aronsen JM, Norden ES, Cataliotti A, Sjaastad I, Sejersted OM, et al. Ryanodine receptor dispersion disrupts Ca<sup>2+</sup> release in failing cardiac myocytes. *Elife*. 2018;7:e39427. doi: 10.7554/eLife.39427
  68. Stefan E, Wiesner B, Baillie GS, Mollajew R, Henn V, Lorenz D, Furkert J, Santamaria K, Nedvetsky P, Hundsrucker C, et al. Compartmentalization of cAMP-dependent signaling by phosphodiesterase-4D is involved in the regulation of vasopressin-mediated water reabsorption in renal principal cells. *J Am Soc Nephrol*. 2007;18:199–212. doi: 10.1681/ASN.2006020132
  69. Schäfer G, Milčić J, Eldahshan A, Götz F, Zühlke K, Schillinger C, Kreuchwig A, Elkins JM, Abdul Azeez KR, Oder A, et al. Highly functionalized terpyridines as competitive inhibitors of AKAP-PKA interactions. *Angew Chem Int Ed Engl*. 2013;52:12187–12191. doi: 10.1002/anie.201304686
  70. Ottesen AH, Louch WE, Carlson CR, Landsverk OJB, Kurola J, Johansen RF, Moe MK, Aronsen JM, Høiseith AD, Jarstadmarken H, et al. Secretoneurin is a novel prognostic cardiovascular biomarker associated with cardiomyocyte calcium handling. *J Am Coll Cardiol*. 2015;65:339–351. doi: 10.1016/j.jacc.2014.10.065
  71. Chang BH, Mukherji S, Soderling TR. Characterization of a calmodulin kinase II inhibitor protein in brain. *Proc Natl Acad Sci U S A*. 1998;95:10890–10895. doi: 10.1073/pnas.95.18.10890
  72. Asensio CJ, Garcia RC. Determination of a large number of kinase activities using peptide substrates, P81 phosphocellulose paper arrays and phosphor imaging. *Anal Biochem*. 2003;319:21–33. doi: 10.1016/s0003-2697(03)00282-3
  73. Witt JJ, Roskoski R Jr. Rapid protein kinase assay using phosphocellulose-paper absorption. *Anal Biochem*. 1975;66:253–258. doi: 10.1016/0003-2697(75)90743-5
  74. Rellos P, Pike AC, Niesen FH, Salah E, Lee WH, von Delft F, Knapp S. Structure of the CaMKII $\delta$ /calmodulin complex reveals the molecular mechanism of CaMKII kinase activation. *PLoS Biol*. 2010;8:e1000426. doi: 10.1371/journal.pbio.1000426
  75. Erickson JR. Mechanisms of CaMKII activation in the heart. *Front Pharmacol*. 2014;5:59. doi: 10.3389/fphar.2014.00059
  76. Horner A, Goetz F, Tampé R, Klussmann E, Pohl P. Mechanism for targeting the A-kinase anchoring protein AKAP18 $\delta$  to the membrane. *J Biol Chem*. 2012;287:42495–42501. doi: 10.1074/jbc.M112.414946
  77. Gray CBB, Brown JH. CaMKII $\delta$  subtypes: localization and function. *Front Pharmacol*. 2014;5:15. doi: 10.3389/fphar.2014.00015
  78. Hou Z, Kelly EM, Robia SL. Phosphomimetic mutations increase phospholamban oligomerization and alter the structure of its regulatory complex. *J Biol Chem*. 2008;283:28996–29003. doi: 10.1074/jbc.M804782200